Babeș-Bolyai University

Cluj-Napoca, Romania

Faculty of Chemistry and Chemical Engineering

Doctoral School of Chemistry

Biocatalytic approaches for the synthesis of optically pure alcohols and amines

PhD Thesis Abstract

PhD Candidate: Cristian Andrei Gal

Scientific Supervisor: Prof. Dr. Csaba Paizs

Cluj-Napoca

2022

Babeș-Bolyai University

Cluj-Napoca, Romania

Faculty of Chemistry and Chemical Engineering

Doctoral School of Chemistry

Biocatalytic approaches for the synthesis of optically pure alcohols and amines

PhD Thesis Abstract

PhD Candidate: Cristian Andrei Gal

President: Prof. Dr. Ion Grosu – corresponding member of the Romanian Academy – Babeș-Bolyai University, Cluj-Napoca, Romania

Scientific Supervisor: Prof. Dr. Csaba Paizs – Babeș-Bolyai University, Cluj-Napoca, Romania

Reviewers: Prof. Dr. Jörg Pietruszka – Heinrich Heine University, Düsseldorf, Germany

Prof. Dr. Francisc Péter – Politehnica Univerisity of Timișoara, Romania

Assoc. Prof. Dr. Anamaria Elena Terec – Babeș-Bolyai University, Cluj-Napoca, Romania

Cluj-Napoca

2022

Table of Contents

1. Introduction

1.1. Role of the biocatalysis in sustainability

Given the fact that in biocatalysis the enzymes are used as catalysts, a perfect match with five principles are met. These features are effects caused by the catalyst itself (enzymes), they can work chemo- region- and enantioselective in the reactions which may be difficult to obtain in chemocatalysis. These catalysts (usually they can bring nearly perfect enantioselectivities) have opened new horizons in the field of catalysis: they are green, profitable, therefore good for the planet and last but not least for the profit as well.[1]

The enzymatic catalysis is usually done under mild conditions (normal pressure and ambient temperature), in water, in standard reactors. In contrast the 80s scientist have demonstrated that the lipases are more thermostable in neat organic solvent (toluene at 100 ˚C) than in water.[2] This work showed the way for how enzymes can be used in organic synthesis. Moreover, the cumbersome protection, deprotection and activation steps of functional groups can be often avoided, thus their use is step economic[3], therefore they are generating fewer waste.

From the sustainability's point-of-view one-pot, multistep processes are really advantageous: minimized solvent usage, maximized space time yields, fewer steps (without derivatization and protecting groups), higher performance, low waste.[4] When enzyme cascades can drive the reaction equilibria towards to the product formation, there is a huge increment in terms of sustainability.[5] Biocatalysis is able to use growing and metabolically active cells.[6] With the ability of this technique, some metabolites can be overproduced such as vitamins, amino acids, alcohols, carboxylic acids.[7] These whole cell systems are practical because the physical protection of the enzymes (offered by the cell wall) are provided, moreover the cofactor regeneration and the easy recovery of the cells can make multistep reactions accessible.

The ACS Green Chemistry Institute's Pharmaceutical Round Table published the key areas of research, where the enzymes can be helpful in integration of green chemistry into pharmaceutical industry.[8] As expected, biocatalysis plays a crucial role in most of these research areas.

1.2. Biocatalysis in flow

Nowadays there are two major trends in the syntheses of APIs: biocatalysis and flow chemistry.[9] [10] One important aspect of the use of flow chemistry is the tremendous potential in terms of the safety of the reactions. Notably, the risks associated with high pressure reactions, the exposure of hazardous chemicals, the heat generated by exothermic reactions can be solved.[11] In correlation with biocatalysis (which generally avoids hazardous chemicals, extreme reaction conditions) the two technologies could have been merged immediately in a really beneficial technology which has not happened in a blink of an eye. Withal, the pharmaceutical industry's regulations are enhancing the use of biocatalysis in the production of APIs, that is the reason why biocatalysis should step into continuous trend as well.[12] In addition to this, the beneficial effects of flow chemistry in a process point of view are more clear.[13] [14] With the practice of flow chemistry, process intensification[15] and integration[16] are easily available and the reaction conditions are uniform, thus the experiments are more controllable. Temperature control can be carried out precisely, pH can be regulated in line, catalysts can be compartmentalized. Compartmentalization is highly important in these classes of catalysis given the fact, that they are more inconsistent than other catalysts.

Flow chemistry can offer solutions for the problems appeared in use of biocatalysts in chemical synthesis. The use of batch stirred tank reactors is not so efficient in the setup in which usually is exploited: vigorous stirring and elevated temperature. These two can lead to fast enzyme inactivation as a result of increased temperature and interfacial effects.[17] The application of biocatalysis in flow chemistry was reviewed meticulously[18] and has been demonstrated its applicability for various substances. The swift development of electronics and artificial intelligence (AI) systems are pronounced in flow chemistry as well, with the possibility for better sensors and control systems.[19]

On **Figure 1** is presented how microfluidic immobilized enzyme reactors (μ-IMER) are usually configured. The configuration can be: serial array cascade (**Figure 1A**) or the biocatalysts can be co-immobilized together (**Figure 1C**) which has the advantages of the enzymes being in a close proximity to each other. Another possibility is to insert another catalyst between the enzyme units (**Figure 1B**).[20]
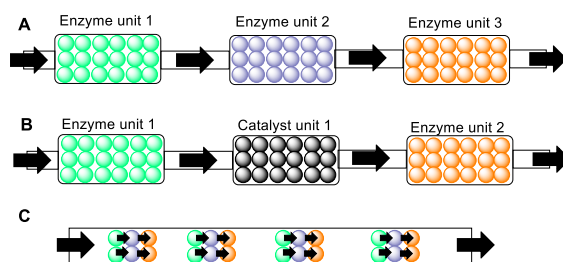
Figure 1. Configurations of *μ*-IMERs

By compartmentalization of the reactions, which is one of the biggest advantage of flow chemistry, some reactions were empowered that otherwise would have been unachievable. The beneficial effect of compartmentalization can be recognized in the synthesis of primary-, secondary amines and in the case of 4'-*O*-methylnorbelladine, which is a precursor for galantamine (dementia drug).[21]

1.3. The use of the enzymes in kinetic resolutions

The growth and the fast development of enzymatic transformations were further accelerated by two societal developments. First, the US Pollution prevention Act[22] (this encouraged the change from "stoichiometric" methodologies to waste prevention because the former generated tremendous amount of waste) and second, the regulatory agencies introduced laws which indicated mandatory tests for each stereoisomers of the chiral drugs.[23] Enzymatic resolutions were limited to kinetic resolutions (KRs), for example amides and esters with hydrolases. This afforded a 50% yield of the desired enantiomer, which will indicate a 50% yield of the unwanted enantiomer (distomer) considered as waste, which has to be racemized in order to recycle it and this, in some cases is performed *in situ*.[24]

1.3.1. Lipases in stereoselective synthesis of chiral alcohols

Presently, enantiomerically pure alcohols are essential building blocks as they are widely needed as intermediates in the pharmaceutical and chemical industries for the syntheses of chiral center containing flavourings, drugs, agrochemicals, liquid crystals and specialty materials.[25] Hence, their synthesis is of great interest to scientists. All in all, the conventional synthetic methods for their enantiomerically pure syntheses are performed mainly with toxic metals or expensive ligands. To circumvent these drawbacks, enzymes are offering a green and sustainable way for their production in an optically pure manner.[26] [27] In traditional organic synthesis methods, enantiomerically pure alcohols lack any knobs for region- and stereo-

control of the reaction. Thus, due to the harsh reaction conditions, undesired side reactions (aldol reaction) and follow-up reactions (dehydration) can occur.[28] Beside these, after catalysis the biocatalysts are easily decomposed by the environment, this makes their use a possible option to conventional chemical synthesis.[29]

The seven major strategies for the enzymatic synthesis of enantiomerically pure alcohols are: 1) enantioselective water addition to α,β-unsaturated ketones, which leads to hydroxyl ketones[30]; 2) enantioselective aldol addition, which produces hydroxyl ketones by an asymmetric carbon-carbon bond formation[31]; 3) enantioselective coupling of ketones or aldehydes with hydrogen cyanide, this leads to nitrile-substituted chiral alcohols (cyanohydrins)[32]; 4) asymmetric reduction of carbonyl compounds[33]; 5) (dynamic) kinetic resolution of racemic mixtures, which is fundamental in the optically pure alcohols[34]; 6) enantioselective hydrolysis of epoxides, which leads to vicinal diols[35]; 7) region- and stereoselective hydroxylation of C-H bonds, to produce the hydroxylated substances[36].

Secondary alcohols are the most generally used substrates in lipase catalyzed KRs. This is a result of high request for this compound class and the elevated enantioselectivity presented by lipases towards secondary alcohols (this is lower towards primary and tertiary alcohols) has helped this technique dissemination.[37] The outcome of KRs is highly predictable, due to the rule of Kazlauskas.[38] Usually the (*R*)-alcohol enantiomer is converted into (*R*)-acetate at a much higher rate (with high enantiomeric excess (ee)). The (*S*)-alcohol, in this way, will remain unreacted. If is desired to recover the (*R*)-alcohol (from (*R*)-acetate), lipase catalyzed hydrolysis is the way to go to obtain the (*R*)-alcohol with high ee thus, the two enantiomers would be separated.

Lipases can be productive catalysts in the KRs of chiral primary amines[39] and on chiral secondary amines as well (although this is not so common)[40], they are acting through enantioselective acetylation of the amino group of the racemic substrate. A favorable ability of lipases is that they remain unreactive towards the hydrolysis of the amide bond (which in the process is formed by this enzyme class), making the amide bond formation irreversible.[41] Diverse parameters have impact on the productivity and selectivity of lipase catalyzed enantioselective amide bond formation, namely solvent type[42], water content of the participating compounds (enzyme preparation, acetyl donor, substrate and solvent)[43] and the activity of the corresponding enzyme (or immobilized enzyme activity, if the aim is to use in continuous flow systems).

1.3.2. ω-transaminases in the stereoselective synthesis of chiral amines

The recent advances in the field of biocatalysis have been also paid off in the synthesis of chiral amines. According to an estimation, 40% of current pharmaceuticals are containing an amine functionality[44], making these compounds relevant building blocks in the pharmaceutical industry. Usually the most widely used method for the chiral amine synthesis is through the hydrogenation of a Schiff-base[45], despite the fact that other methods have also been engaged such as, nucleophilic addition, C-H insertion and diastereoisomeric crystallization. For the green and sustainable production of this compound class, enzymatic synthesis strategies have been considered with hydrolases[46], while other enzymes were taken into consideration for the synthesis of this important substance class such as: oxidazes, lyases and transaminases (TAs).[47]

TAs are the enzymes which are transferring the amino functional group, from an amino donor molecule to an amino acceptor molecule, which is usually a ketone or an aldehyde.[44] They are cofactor dependent enzymes, their cofactor is the PLP which arbitrate the previously mentioned reaction.[48] This reaction in nature is commonly represented by the transfer of the amino moiety from an α-amino acid to an α-keto acid, underlining their principal role as biocatalyst. Besides this, they are possesing the universal phenomenon of nitrogen assimilation of all organisms.[49][50] In the last decade a considerable number of reviews[51][52][53] have presented the potential carried out by these enzymes, underlying their pivotal role in the production of chiral amines and amino acids.[54] In the late 1980's the reactions catalyzed by TAs have already been adopted on industrial scale biocatalysis for the production of optically pure amines, in both KR setup and in asymmetric synthesis too.[55] Both (*R*)- and (*S*)-selective TAs, working in asymmetric synthesis on prochiral ketones, have been developed. At the beginning of the next decade this practice was elevated onto a higher level in the academic environment.[56][57]

2. Aims of the study

The presented thesis has the aim to offer **efficient methods towards the synthesis of optically pure alcohols and amines**. To fulfill the targeted point, the following objectives needs to be successfully realized:

Objective 1. Flow production of enantiopure secondary alcohols with immobilized lipase B from *Candida antarctica* (CaL-B).

Covalent immobilization of CaL-B (**a**). This will enable its use in continuous flow mode to obtain enantiopure alcohols. **Flow biocatalysis with CaL-B** the creation and optimization of a system to obtain, in neat organic solvent, optically pure secondary alcohols in preparative scale (**b**) (**Figure 2.**).
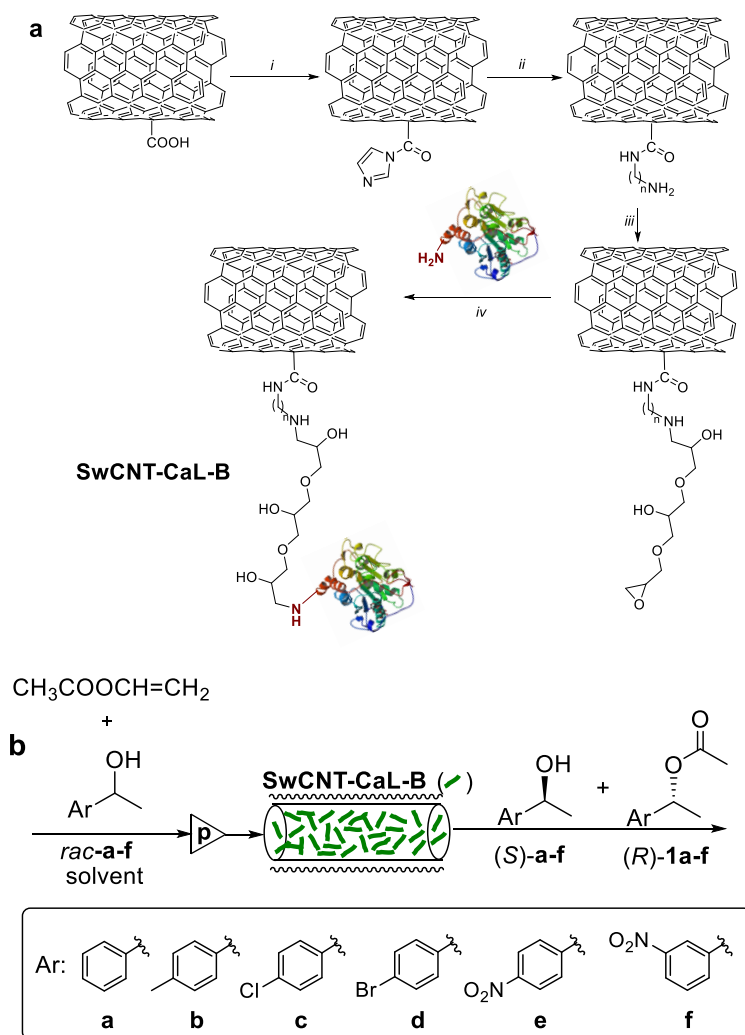
Figure 2. The envisaged immobilization strategy for the lipase (**a**); the projected system for the kinetic resolution of secondary arylethan-1-ols in continuous flow mode (**b**)

Objective 2. Lipase in dynamic kinetic resolution of amines.

Creation of a continuous flow system for the efficient DKR of various benzylic amines (**Figure 3.**).
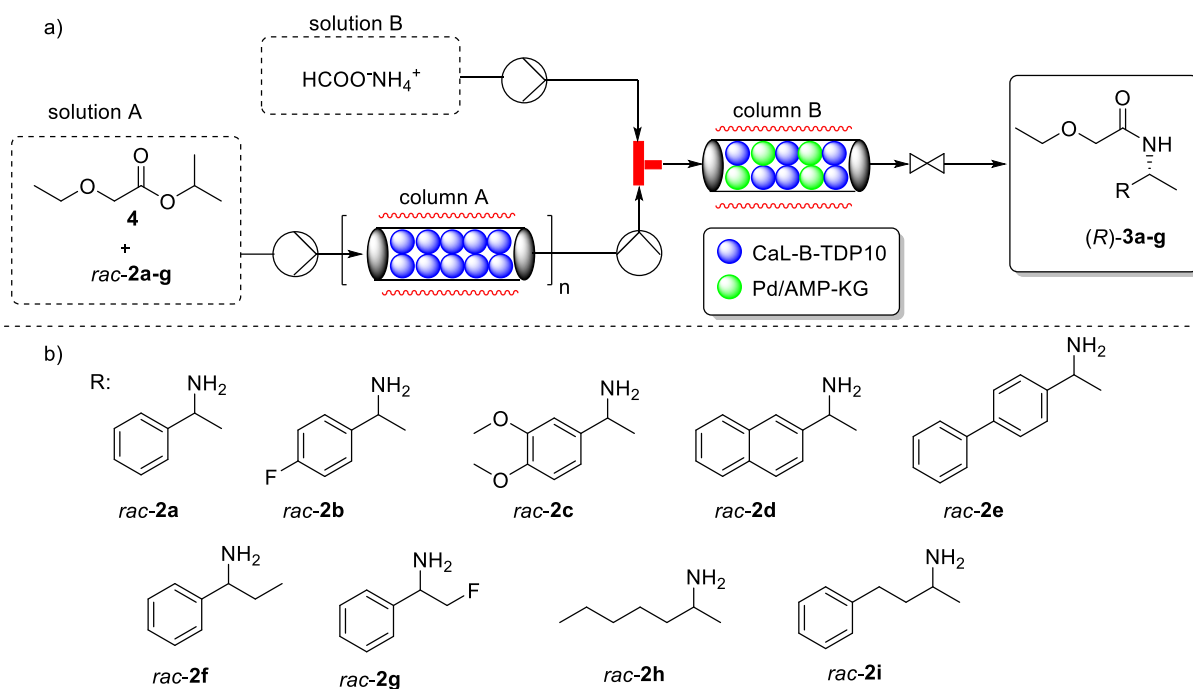
Figure 3. The desired system for the DKR of amines

Objective 3. TAs for the production of (*R*)- and (*S*)-amines.

It was aimed to characterize two, unknown by the literature, TAs for the KR of amines in batch mode. Furthermore, it was planned to compare their catalytic properties to one, previously well studied TA (**Figure 4.**).
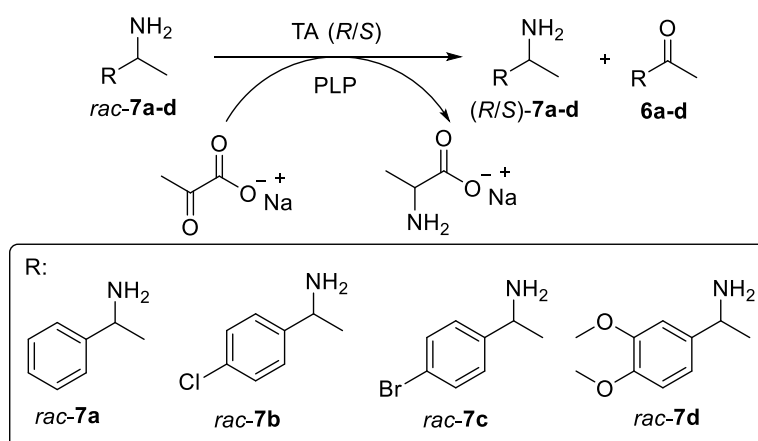
Figure 4. Kinetic resolution catalysed by TAs

3. Results and discussion

3.1. Immobilization procedure for lipase B from *Candida antarctica* (CaL-B)

3.1.1. Covalent immobilization of the lipase on single-walled carbon nanotubes (SwCNT)

N,N'-carbonyldiimidazole was used to activate the carboxy functionalized carbon nanotubes ($SwCNT_{COOH}$). Afterwards the activated nanotubes were reacted with α,ω-diaminoalkanes (with different chainlenghts: C_3- C_6- C_8-), producing aminoalkyl functionalized SwCNTs with increasing chainlenght: $SwCNT_{COOH}$-C_3-NH_2, $SwCNT_{COOH}$-C_6-NH_2 and $SwCNT_{COOH}$-C_8-NH_2. These structures were further reacted with glycerol diglycidyl ether (GDE). CaL-B was covalently immobilized (nearly in quantitative yield) to this support, with free enzyme:support *ratio* 1:2 (w/w), in the latency of Tween 80 (non-ionic surfactant) it has been obtained three immobilized enzyme arrangements ($SwCNT_{COOH}$-C_n-NH-GDE-CaL-B; n=3, 6, 8). To prove the method, every immobilization was carried out in triplicate and the resulting biocatalysts were probed in the model reactions (acetylation of *rac*-phenylethan-1-ol in the presence of vinyl acetate in n-hexane solvent) in order to get a feedback on the enzyme activity and stereoselectivity, after being immobilized to the carbon support. After the reactions being followed in time, it has been revealed that the immobilization procedure is highly reproducible and the catalytic efficiency drops with the growing alkane chain length (used as spacer in immobilization). All biocatalysts presented excellent stereoselectivity, the best performance was noticed in the model reaction with $SwCNT_{COOH}$-C_3-NH-GDE-CaL-B ($SwCNT_{COOH}$-CaL-B) (**Figure 5.**).
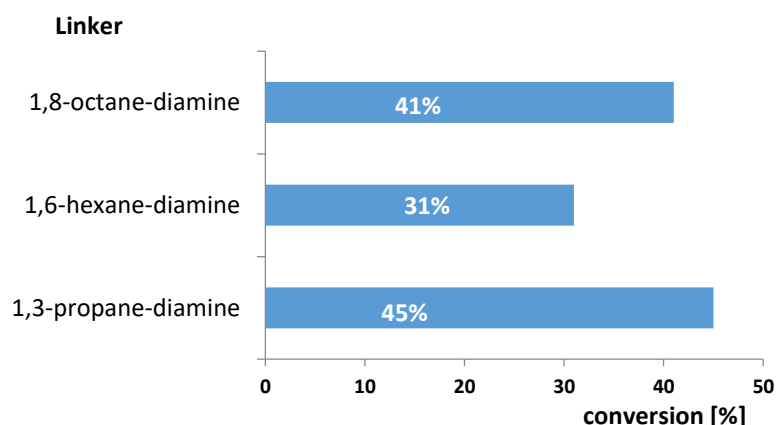
Figure 5. The influence of the spacer length on the activity of KR (enzyme:support *ratio* 1:2, 0.75 equiv. vinyl acetate, *n*-hexane, 30°C, after 2 hours)

The immobilization procedure to obtain the covalently immobilized lipase was performed by a method previously developed by our group,[58 59] presented on **Figure 6.**
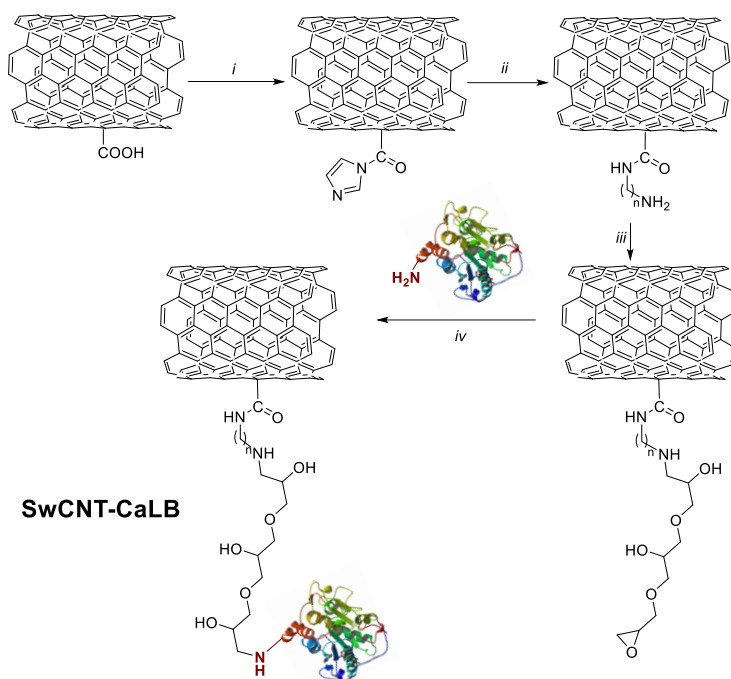
Figure 6. Covalent immobilization of CaL-B on SwCNT$_{COOH}$

3.1.2. The importance of the enzyme loading on the support material

The catalytic performance of the immobilized biocatalyst was investigated in a reaction of the model substrate's, *rac*-phenylethan-1-ol (*rac*-**a**), enantioselective acetylation with vinyl acetate in *n*-hexane at 30 °C for a reaction time of 1 hour (**Table 1.**). The catalysts were precisely weighed, to ensure the same amount of SwCNT-CaL-B in the reaction mixtures.

Table 1. The effect of enzyme loading on the activity of the immobilized biocatalysts (2 mg *rac*-**a** /mL, 0.75 equiv. vinyl acetate, in *n*-hexane as solvent, at 30 °C, after 1 h)

Entry	Support-Enzyme *ratio* (w/w)	Enzyme loading (mg CaL-B/mg support)	c (%)
1	4:1	0.16	41
2	2:1	0.33	42
3	1:1	0.5	41
4	1:2	0.66	42
4	1:3	0.72	35
5	1:4	0.78	29
6	1:5	0.83	24

It was identified that the enzyme:support ratio in the range from 1:4 to 2:1 (w/w) produced nearly identical specific activities. The higher enzyme loading was not beneficial to specific activity, thus in SwCNT-CaL-B the enzyme:support ratio (w/w) 2:1 was preferred for the following experiments, as this is the most cost effective variant of the enzyme-support preparations.

3.2 Flow biocatalysis with CaL-B

3.2.1. Chemical synthesis of alcohols and acetates

The chemical synthesis of racemic secondary alcohols (*rac*-**a-f**) was performed by ketone reduction with $NaBH_4$. Chemical synthesis of the racemic acetylated alcohols (*rac*-**1a-f**) was achieved with acetyl chloride in the presence of 4-Dimethylaminopyridine (DMAP). For the structural confirmation of *rac*-**a-f** and *rac*-**1a-f** ^{1}H- and ^{13}C-NMR measurements were carried out. Moreover, chiral HPLC- or GC-parameters were established for the baseline separation of the afformentioned substances.

3.2.2. The influence of the organic solvents on lipase activity

The SwCNT-CaL-B was tested in many organic solvents, such as aromatic, aliphatic and halogenated hydrocarbons, ethers and nitriles. In the acetylation reaction, for substrates *rac*-**a-d** the *n*-hexane has proven to be the best choice in terms of catalytic efficacy (velocity

and stereoselectivity). The same screening, in the case of *rac*-**e-f** gave different results, in this comparison DIPE has proven to be the best choice for the enantioselective (*E*) acetylation of secondary alcohols (**Table 2.**).

Table 2. Solvents for optimal biocatalytic kinetic resolution of *rac*-**a-f** (2 mg *rac*-**a-f**/mL, 0.75 equiv. vinyl acetate, 1.5 mg catalyst, 500 μL solvent, at 30 °C)

Substrate	Solvent	Time (h)	ee_S (%)	ee_P (%)	c^a (%)
rac-**a**	*n*-hexane	2	99	99	50
rac-**b**	*n*-hexane	4	99	99	50
rac-**c**	*n*-hexane	4	99	99	50
rac-**d**	*n*-hexane	6	98	99	50
rac-**e**	DIPE	8	98	99	50
rac-**f**	DIPE	8	99	99	50

[a] Enantiomer selectivity was excellent (*E* >>200) in all cases.

3.2.3. Temperature profile screening of SwCNT-CaL-B in enantioselective acetylation

For further experiments the effect of the temperature on the model substrate (*rac*-**a**) was investigated in *n*-hexane, between 30-60 ˚C. At this point, the transformations were performed in batch mode, with sampling after 1 h reaction time at different temperatures. The set reaction parameters (were substrate concentration, SwCNT-CaL-B amount, acetylating agent amount and solvent) resulted the best temperature to be at 60 ˚C for the KR, where the conversion was close to maximal (theoretically possible - 50%) value. As it has been anticipated, a catalytic enhancement was recognized with the increase of temperature, however the lipase has not performed well near 40 ˚C, this is in good concordance with the observations made on this fact in previous works.[58] The rise of temperature decreased the viscosity of the system, thus the diffusion process was enhanced[60] and the substrate accessibility to the catalytic microenvironment of the enzyme (**Figure 7.**).
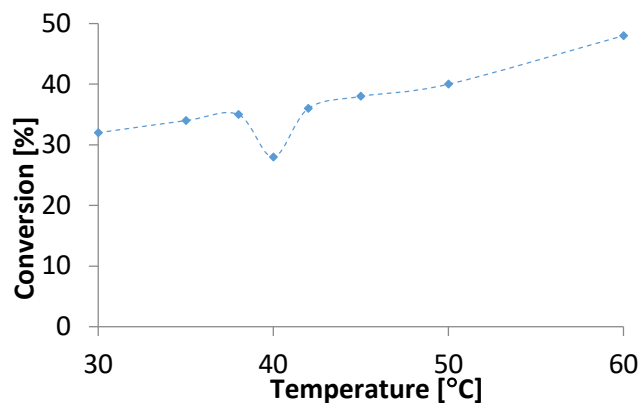
Figure 7. The conversion profile of the biocatalyst at varied temperatures in the reaction of *rac*-**a** (2 mg/mL) with vinyl acetate (0.75 equiv.) in *n*-hexane, 3 mg SwCNT-CaL-B, after 1 h reaction time

3.2.4. Recyclability of SwCNT-CaL-B in batch mode

The recyclability of the best performing immobilized lipase preparation (0.66 mg lipase / mg biocatalyst) was investigated with the model substrate (*rac*-**a**) in consecutive batch reactions under the previously set reaction conditions (2 mg/mL substrate in *n*-hexane, 0.75 equiv. vinyl acetate, 60 ˚C). The SwCNT-CaL-B maintained its initial activity even after 10 consecutive reaction cycles, proven in this way its possibility to be used under preparative scale kinetic resolution of arylethane-1-ols (**Figure 8.**).
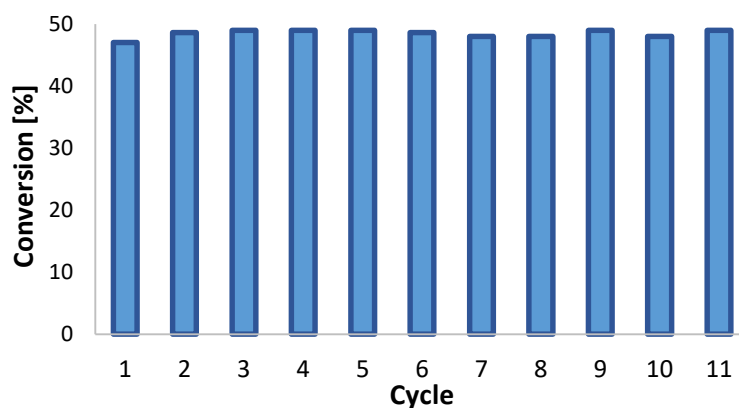
Figure 8. The conversions produced by the biocatalyst after 1 h reaction time in repeated reaction cycles

3.2.5. Continuous flow lipase catalyzed acylation of *rac*-**a**

The reactor was completely filled with dry biocatalyst under vacuum. The closed reactor was placed vertically and *n*-hexane was pumped through from the bottom of the reactor.

16

After the air was flushed out from the reactor, the compressibility of the biocatalyst bed was tested. In order to perform this test, the hexane flow rate was increased gradually from 0.1 to 5 mL/min, causing a growing pressure-drop on the reactor, just with ~1.5 bar. Consequently the reactor was inversly attached and the same experiment was preformed (increase of hexane's flow rate), concluding the same results as observed before with the same pressure drop over the flow-rate. After it has been inspected visually, no compression of the catalyst bed was marked.

3.2.5.1. The influence of temperature and substrate concentration on the enzymatic acylation of model substrate (*rac*-**a**) in flow-mode

In this set of experiments, it was aimed to investigate the influence of temperature upon the SwCNT-CaL-B catalyzed acylation of *rac*-**a** (2 mg/mL) with vinyl acetate (0.75 equiv.). In concordance with the experiment done in batch setup, in this case the temperature range was varied from 30 ˚C to 60 ˚C, exposing the same decrease of activity around 40 ˚C (**Figure 9.**).
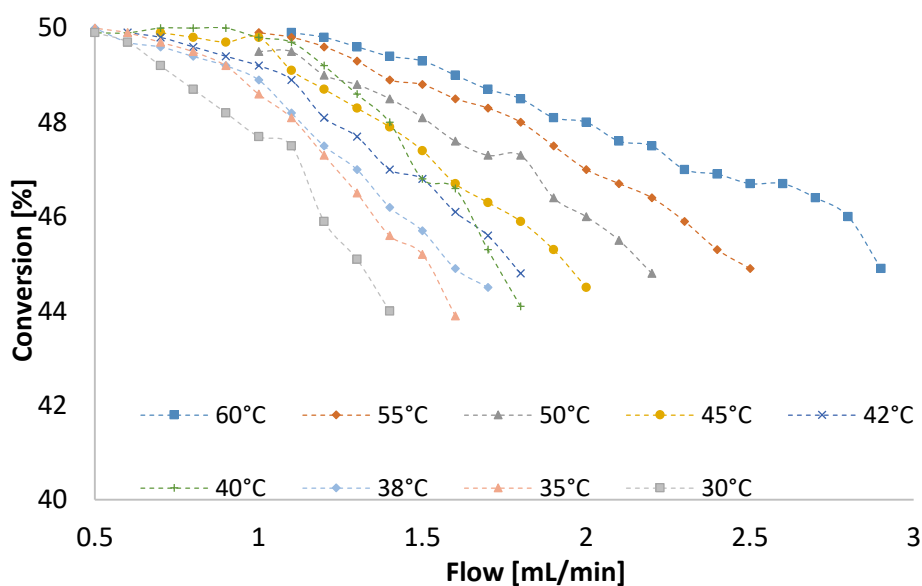
Figure 9. The catalytic performance of SwCNT-CaL-B in the KR of *rac*-**a** (2 mg/mL) with vinyl acetate (0.75 equiv.) at various temperatures in *n*-hexane, in continuous-flow mode

In the following, it was aimed to enhance the productivity of the continuous-flow kinetic resolution system. For this aim, the *rac*-**a** concentration was elevated (to 10, 20, 30, 40 and 50 mg/mL) (vinyl acetate 0.75 equiv.) and it was investigated the substrate concentration influence on the conversion at various flow rates (0.1-1 mL/min) and temperature (30-60 ˚C) values (**Figure 10A-E.**).

A

B

C

D
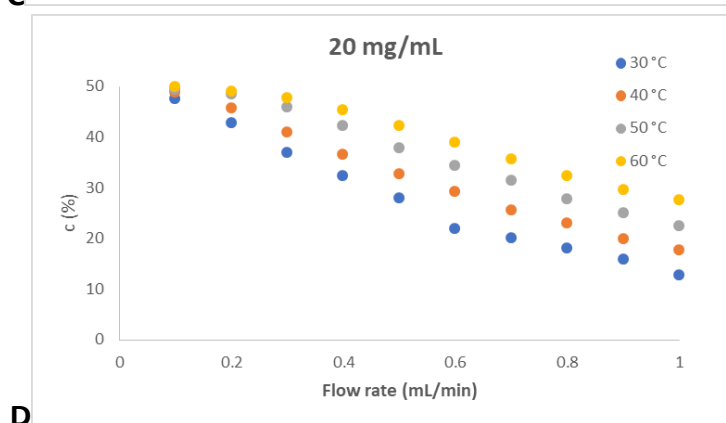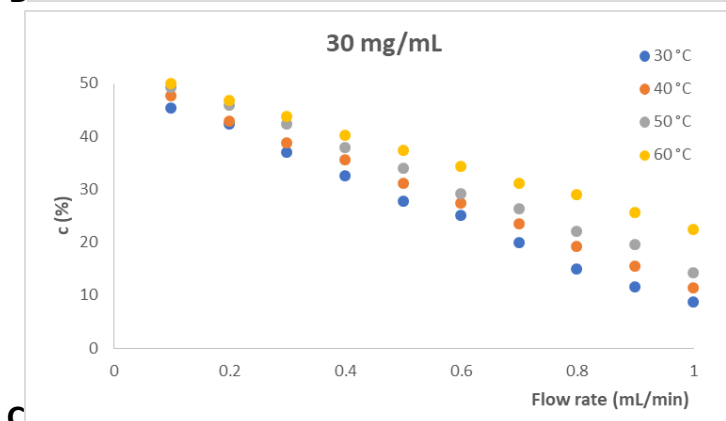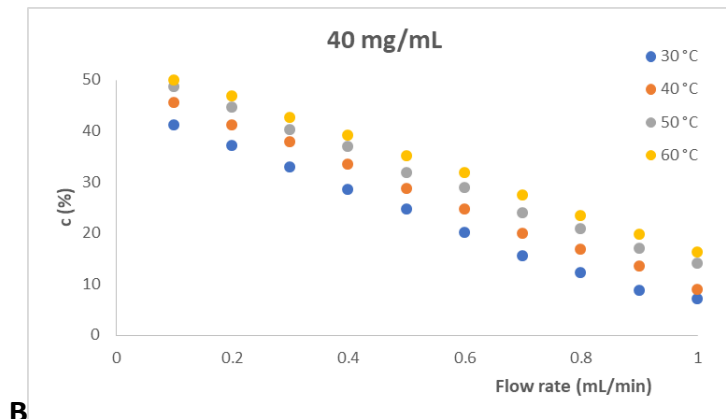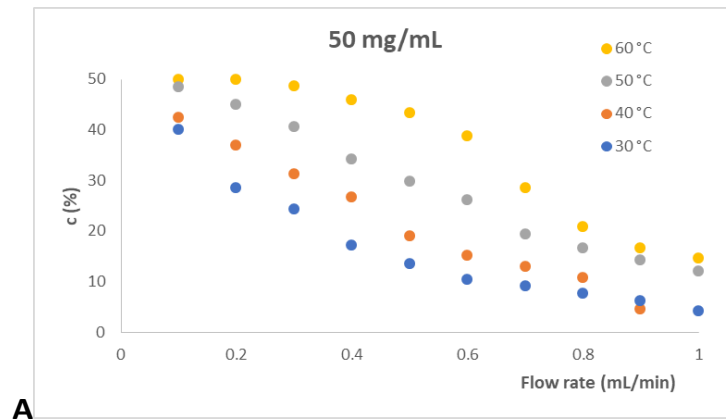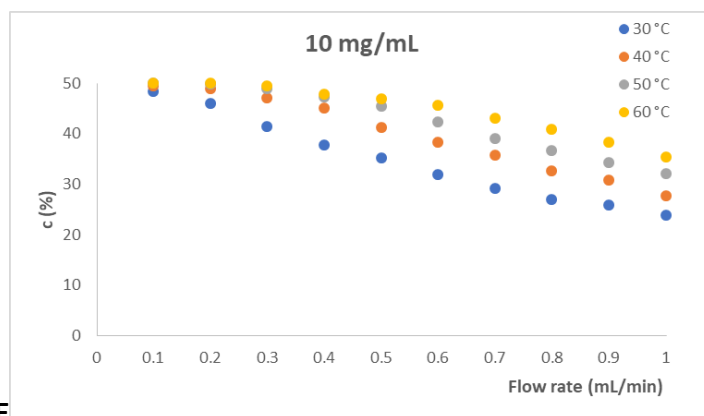
Figure 10A-E. The effect of the flow rate at various substrate (*rac*-**a**) concentrations (50, 40, 30, 20 and 10 mg/mL) and temperatures (30, 40, 50 and 60 ˚C) on the conversion (*c*) of the continuous flow kinetic resolution. Reaction conditions: 70 mg SwCNT-CaL-B, *n*-hexane, 0.75 equiv. vinyl acetate

3.2.5.2. Lipase catalized acylation of *rac*-**a-f** in continuous flow setup

To demonstrate the broad applicability of SwCNT-CaL-B, the experience gained in batch reaction setup for *rac*-**c-f** was transferred to flow setup. Due to the structural closeness between *rac*-**a** and *rac*-**b**, the methyl substituted phenylethan-1-ol was excluded from the flow experiments. The *para*-halogenated-alcohols (*rac*-**c,d**) were suitable substrates for the immobilized CaL-B (**Figure 11A.**), the kinetic resolution of nitro-phenylethan-1-ols (*rac*-**e-f**) appeared to be slower, which is reflected in the lower flow rates necessary to obtain the desired conversions (**Figure 11B.**).
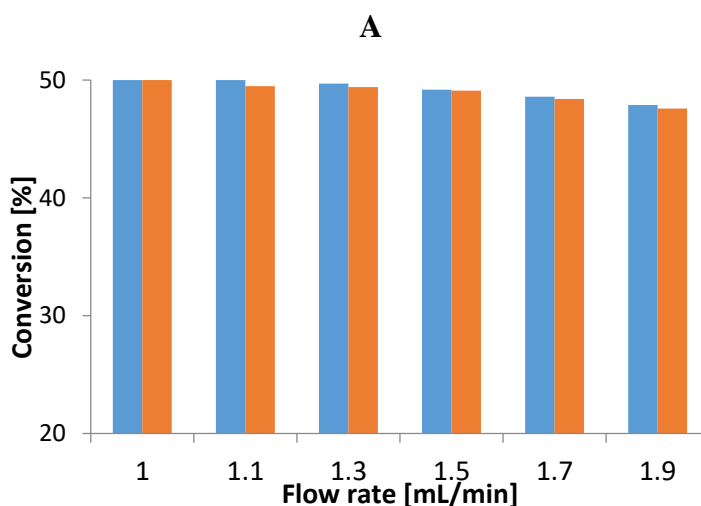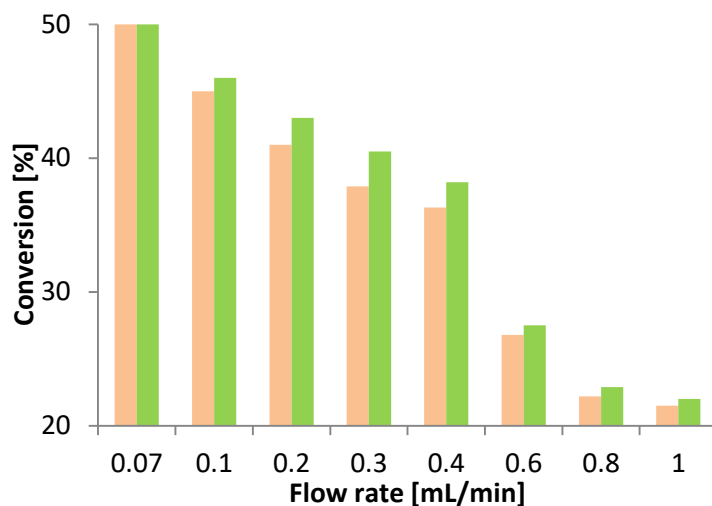
Figure 11. Continuous-flow acylation of (**A**): *rac*-**c** (blue bars) and *rac*-**d** (red bars) and (**B**): *rac*-**e** (orange bars) and *rac*-**f** (green bars) with SwCNT-CaL-B. Reaction conditions:, the previously defined organic solvent, 0.75 equiv. vinyl acetate, 2 mg/mL *rac*-**c-f**, 60 °C, 70 mg SwCNT-CaL-B

The productivity (r_{flow}, μmol/mL × mg) of the system with the best performing biocatalyst (SwCNT-CaL-B) was calculated for the kinetic resolution of the model substrate (*rac*-**a**) for all five concentrations (10, 20, 30, 40 and 50 mg/mL) and at all four temperatures (30, 40, 50 and 60 °C) in the flow rate range from 0.1 – 1 mL/min (**Figure 12.** and Equation (1)).

$$r_{flow} = \frac{[P] \times f}{m_e} \left[\frac{\mu mol}{min \times mg}\right] (1)$$
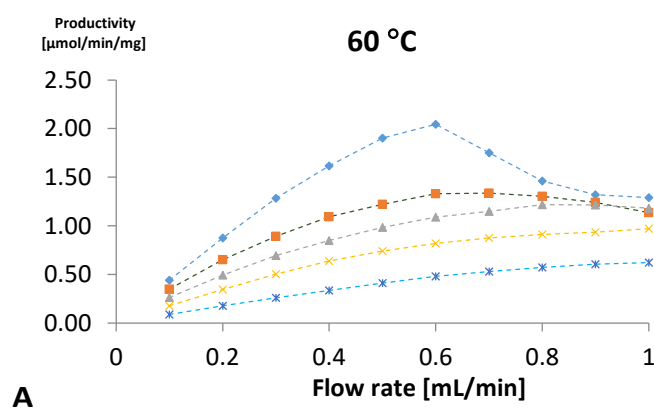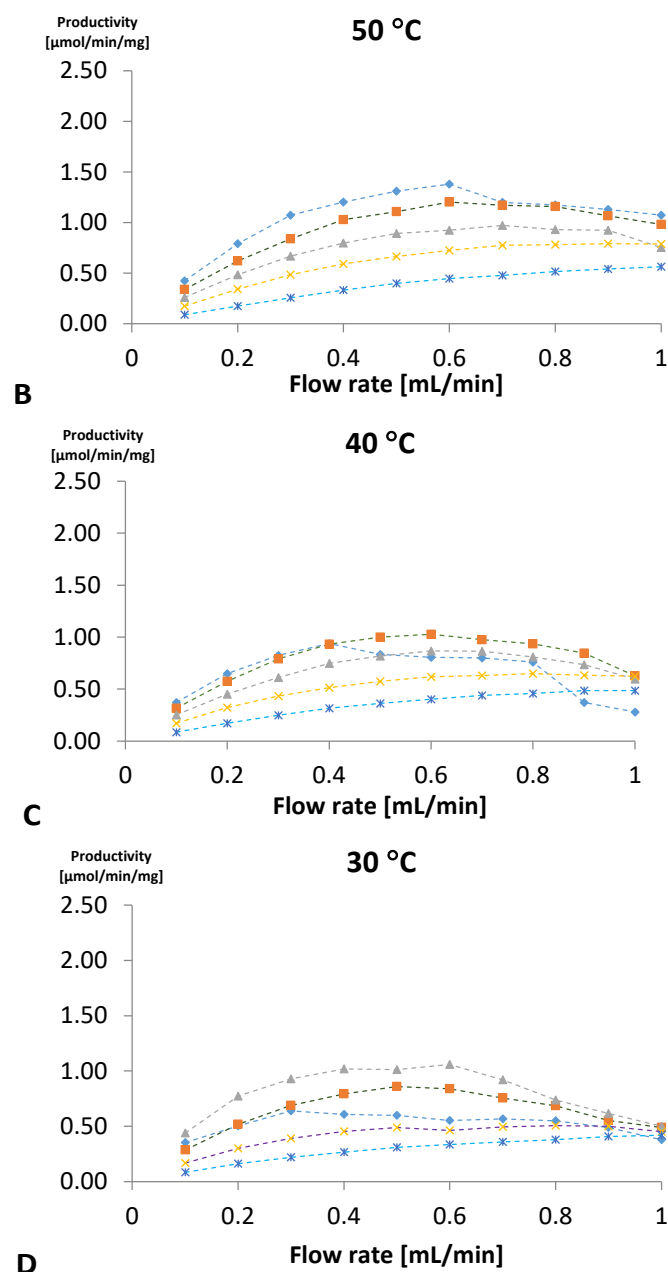
Figure 12. The variation of productivity ($\mu mol_{product}$ min^{-1} mg^{-1} biocatalyst) of SwCNT-CaL-B in function of flow rate at different temperature and substrate concentrations (♦ 50 mg mL^{-1}; ■ 40 mg mL^{-1}; ▲ 30 mg mL^{-1}; × 20 mg mL^{-1}; ✳ 10 mg mL^{-1}).

In Equation (1), m_e is the weight of the biocatalyst in the reactor (in mg), [P] is the (R)-**1a** concentration (given as $\mu mol/mL$, calculated from substrate concentration and conversion) and f is the flow rate (mL/min).

The system productivity maximum was calculated to be at 60 °C, with model substrate concentration of 50 mg/mL at a flow rate of 0.6 mL/min. It was determined as 2.04

μmol/mL/mg. On **Figure 13.** it can be followed the system productivity as a function of flow rate, substrate concentration and temperature.
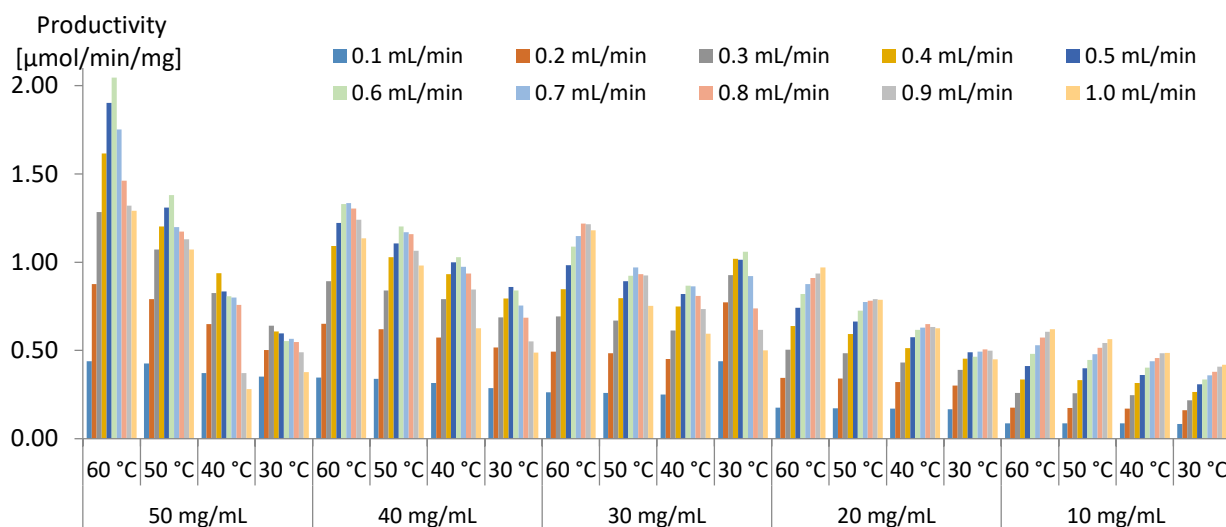
Figure 13. The SwCNT-CaL-B system's productivity

The continuous flow acylation progressed with excellent enantioselectivity in all experiments, providing the product with maximal enantiomeric excess ($ee_p > 99\%$).

3.2.6. Conclusions

In this study, an efficient applicability of the covalent immobilization on functionalized single walled carbon nanotubes of lipase B from *Candida antarctica* has been demonstrated. The aforementioned catalyst was active and selective in both continuous flow and batch modes for the enzyme catalyzed kinetic resolution of different secondary aryl alcohols. The experimental proofs that the results gained by the SwCNT-CaL-B were highly reproducible, regarding activity and stereoselectivity. The presented optimized procedure with elevated productivity was appropriate for the production of enantiopure alcohols and acetates. The ~70 mg biocatalyst loaded into reactor, allowed the hundred-gram scale kinetic resolution of the targeted enantiomers, emphasizing in this way the long term operational stability of SwCNT-CaL-B.

3.3. Lipase in dynamic kinetic resolution of amines in continuous flow

3.3.1. Racemization experiments

Besides the commercially available 10% Pd/C six additional heterogeneous catalysts were produced and tested as racemization agent: Pd/BaCO$_3$,[61] Pd/Al(O)OH,[62] Pd/BaSO$_4$, Pd/AMP-D, Pd/AEAP-D, and Pd/AMP-KG (on in-house produced 3-aminopropyl- and 3-(2-aminoethylamino)propyl-modified silica[63]) carriers. The racemization experiments were performed with the aforementioned catalysis in stainless steel reactors. In the first series of racemization attempts, the microreactors were packed with different catalysts and a solution of (S)-1-phenylethylamine (S)-**2a** and ammonium formate (used as hydrogen source), which together were pumped through the reactor at elevated temperatures (60, 90 and 120 ˚C). In all cases, the racemization experiments were followed and from effluent enantiomeric composition [$ee_{(S)\text{-}2a}$] of **2a** and selectivity ($sel_{(R,S)\text{-}2a}$) were determined. At 120 ˚C the selectivity of Pd catalysts were low ($sel_{(R,S)\text{-}1a} < 5\%$). In 90 ˚C tests slightly improved racemization degrees ($ee_{(S)\text{-}2a} < 15\%$) and selectivities ($sel_{(R,S)\text{-}2a} = 2\text{–}74\%$) can be observed (**Table 3.**).

Table 3. Racemization of (S)-**2a** catalyzed by supported Pd-catalysts in packed-bed continuous-flow reactor at 90 ˚C

entry	catalyst	$ee_{(S)\text{-}2a}$ (%)[a]	$sel_{(R,S)\text{-}2a}$ (%)[a,b]
1	Pd/BaSO$_4$	-	-
2	10% Pd/C	>99	2
3	Pd/BaCO$_3$	13	41
4	Pd/AlO(OH)	4	98
5	Pd/AEAP-D	2	74
6	Pd/AMP-D	<1	9

[a]Determined by GC. [b]$sel(R,S)$-**2** (%)=amount of (R,S)-**2a**/amount of detectable compounds in reaction mixture $\times$ 100.

Given the fact, that temperatures below 70 ˚C were found to be compatible with immobilized *Candida Antarctica* (*Ca*LB)[64], the most thorough racemization studies were performed at this temperature (**Table 4.**, entries 1-7).

Table 4. Racemization results for (*S*)-**2a**, (*S*)-**2h** and (*S*)-**2i** supported by Pd-catalysts in packed-bed continuous-flow reactor using ammonium formate as hydrogen source[a]

entry	amine	catalyst[b]	$ee_{(S)\text{-}2a}$ (%)[c]	$sel_{(R,S)\text{-}2a}$ (%)[c,d]
1	(*S*)-**2a**	10% Pd/C	>99	13
2	(*S*)-**2a**	Pd/AlO(OH)	57	99
3	(*S*)-**2a**	Pd/AEAP-D	36	95
4	(*S*)-**2a**	Pd/BaCO$_3$	6	66
5	(*S*)-**2a**	Pd/BaSO$_4$	1	68
6	(*S*)-**2a**	Pd/AMP-D	5	90
7	(*S*)-**2a**	Pd/AMP-KG	2	94
8	(*S*)-**2a**	Pd/AMP-KG[e]	3	95
9	(*S*)-**2h**	Pd/AMP-KG[e]	99	93
10	(*S*)-**2i**	Pd/AMP-KG[e]	99	90

[a] Entries 1-7: (*S*)-**2a** (69 mM), ammonium formate (1.0 equiv., 69 mM) in dry 2-methyl-2-butanol at 60 ˚C with 20 µL min^{-1} flow rate; Entries 8-10: (*S*)-amine [(*S*)-**2a**, (*S*)-**2h** or (*S*)-**2i**: (69 mM), ammonium formate (1.2 equiv., 83 mM) in dry 2-methyl-2-butanol at 60 ˚C with 10 µL min^{-1} flow rate. [b] Catalyst filling weights available in thesis. [c] Determined by GC. [d] $sel_{(R,S)\text{-}1}$= amount of (*R,S*)-2/amount of detectable compounds in reaction mixture $\times$ 100 (%). [e] Entries 8-10: see catalyst filling weights in thesis.

At 60 ˚C 10% Pd/C converted (*S*)-**2a** chiefly to by-products ($sel_{(R,S)\text{-}2a}$= 13%) without racemization ($ee_{(S)\text{-}2a}$ > 99%; Table 1, entry 1). Interestingly with the other Pd-catalysts (**Table 4**, entries 2-7) various degree of racemization ($ee_{(S)\text{-}2a}$= 1–57%) and selectivity ($sel_{(R,S)\text{-}2a}$= 66-99%) could be obtained. All over, Pd/AMP-KG is proven to be the most useful racemization catalyst at 60 ˚C ($ee_{(S)\text{-}2a}$ = 2%) with good selectivity ($sel_{(R,S)\text{-}2a}$= 94%; **Table 4**, entry 7).

Next, the mixture of a robust sol-gel immobilized form of lipase B from *Candida antarctica* (*Ca*LB-TDP10) was tested with the most encouraging racemization agent (Pd/AMP-KG) in a mixed-bed reactor (column B). It was desired to check the compatibility of the racemization with the immobilized enzyme. In screening, the racemization of (*S*)-**2a** and two non-benzylic amines (*S*)-**2h** and (*S*)-**2i** were tested. The tests revealed smooth and efficient racemization of (*S*)-**2a** with Pd/AMP-KG even in the presence of *Ca*L-B-TDP10 ($ee_{(S)\text{-}2a}$ = 3% with $sel_{(R,S)\text{-}2a}$= 95%: entry 8 in **Table 4.**), yet the non-benzylic amines could not be racemized ($ee_{(S)\text{-}2a}$ $\geq$ 99%: entries 9,10 in **Table 4.**). Because of the occurrence of reductive amination of

non-benzylic amines with Pd-catalysts (with the help of ammonium formate) at even 40 ˚C, poor oxidation may be the reason of non-existent racemization of non-benzylic amines.

To name all obstacles aroused during the preliminary experiments for continuous-flow DKR of 1-phenylethaneamine *rac*-**2a** (see Section 5.2), the coming key elements were used in the final DKR system [n= 1 or 2 in **Figure 14.**, panel b)]: *i)* in the enzyme-catalyzed step isopropyl 2-ethoxyacetate (**4**) was selected as an efficient amine acylating agent; *ii)* a KR column (column A, filled only with *Ca*LB-TDP-10) was introduced to minimize the amount of forming 2-ethoxyacetamide (**5**); *iii)* Pd/AMP-KG (racemization catalyst); *iv)* 2-methyl-2-butanol was replaced with a 2-methyl-2-butanol/toluene 1:1 (v/v) mixture (to enhance the solubility of the more hydrophilic amines *rac*-**2c-e** in solution A); *v)* back pressure was applied at the outlet of column B; *vi)* the column B (Pd/AMP-KG) was pre-activated by a flow of ammonium formate solution (for 30 min).

In the previously described system, on the KR column (column A: *Ca*LB-TDP-10) the solution A (*rac*-**2a** and **4**) was pumped through. The effluent (contained almost equimolar amounts of the amide (*R*)-**3a** and the unreacted amine (*S*)-**2a**) was unified with solution B (ammonium formate in dry 2-methyl-2-butanol) in a three-way valve leading towards a mixed-bed column (column B: Pd/AMP-KG+*Ca*LB-TDP10). It has been examined the effect of imidazolium formate as hydrogen source (**Table 5.**), and equivalency of ammonium formate on DKR of *rac*-**2a** (**Table 6.**).

Table 5. Hydrogen source optimization in DKR of *rac*-**2a** in fully continuous-flow mode[a]

entry	acylating agent[b] (mM) [equiv.]	H-source[c] (mM) [equiv.]	c (%)[d]	Y (%)	ee$_{(R)-3a}$ (%)[d]
1	180 [2.0]	AF, 54 [0.6]	>99e	91	99.6
2	180 [2.0]	IF, 54 [0.6]	>99	90	97.5
3	180 [2.0]	IF, 27 [0.3]	80	75	97.7
4	135 [1.5]	IF, 54 [0.6]	>99	90	98.4
5	108 [1.2]	IF, 54 [0.6]	>99	91	98.3

[a]Conditions – filling weights: column A: M540-CaLB (209 mg), column B: M540-CaLB (120 mg) mixed with Pd/AMP-D (120 mg); flow rates: 5-5 µL min^{-1}; at 60 ˚C. b) Solution A: *rac*-**2a** (90 mM) and isopropyl 2-ethoxyacetate (**4**) in dry 2-methyl-2-butanol. c) Solution B: hydrogen source AF: ammonium formate, IF: imidazolium formate [indicated equivalent to *rac*-**2a**] in dry 2-methyl-2-butanol. d) Determined by GC. e) Formation of 2-ethoxyacetamide (**5**) was observed.

Table 6. Optimization of excess of ammonium formate in DKR of *rac*-**2a** in fully continuous flow mode[a]

entry	HCOONH$_4$ (equiv.)	$ee_{(S)\text{-}2a}$ (%)[b]	$ee_{(R)\text{-}3a}$ (%)[b]	conv. (%)[b]	yield (%)
1	0.2	n.d.[c]	99.9	>99	63
2	0.3	n.d.[c]	99.9	>99	88
3	0.4	n.d.[c]	99.9	>99	92
4	0.6	n.d.[c]	99.9	>99	96

[a] Solution A: *rac*-**2a** (138 mM) and **4** (2 equiv., 276 mM) in dry 2-methyl-2-butanol/toluene 1:1 (v/v) at 5 μL min^{-1} and Solution B: ammonium formate in 2-methyl-2-butanol at 5 μL min^{-1} at 30 psi, 60 ˚C. [b] Determined by GC. [c] Not detected.

The most potent setup for DKR of *rac*-**2a** (temperature: 60 ˚C; flow rate: 5 μL min^{-1} in all pumps, 0.6 equiv. of ammonium formate) delivered (*R*)-**3a** in high isolated yield (96%) with excellent enantiomeric excess (>99%) (**Table 7**, entry 1).

Table 7. Chemoenzymatic DKR of seven benzylic amines, *rac*-**2a-g** in fully continuous-flow mode[a]

entry[a]	amine	n (-)	T (°C)	p (psi)	$ee_{(S)\text{-}2a\text{-}f}$ (%)[b]	$ee_{(R)\text{-}3a\text{-}f}$ (%)[b]	conv. (%)[b]	yield (%)
1	*rac*-**2a**	1	60	30	n.d.[c]	99.9	>99	96
2	*rac*-**2b**	1	60	30	92.0	99.5	61.9	60
3	*rac*-**2c**	2	60	30	63.3	98.9	63.5	60
4	*rac*-**2d**	1	60	30	8.3	99.3	96.7	86
5	*rac*-**2e**	2	60	30	74.4	99.2	65.0	57[d]
6	*rac*-**2f**	1	60	30	9.7	99.9	72.0	67
7	*rac*-**2g**	0[e]	70	100	98(59)[f]	99.1(99.3)[g]	63(75)[h]	n.i.[i]

[a] Entries 1-6: Solution A: *rac*-**2a-f** (138 mM) and **3** (2 equiv., 138 mM) in dry 2-methyl-2-butanol/toluene 1:1 (v/v) at 5 μL min^{-1} and Solution B: ammonium formate (0.6 equiv.) in 2-methyl-2-butanol at 5 μL min^{-1}. [b] Determined by GC (for details, see thesis). [c] Not detected. [d] 4-Ethyl-1,1'-byphenyl was isolated as by-product. [e] Entry 7 (n= 0): no column A, *rac*-**2g** (138 mM), **4** (2 equiv., 138 mM) and ammonium formate (0.6 equiv.) in dry 2-methyl-2-butanol was fed directly to column B at 10 μL min^{-1}. [f] $ee_{(S)\text{-}2g}$ (the value of $ee_{(S)\text{-}2a}$ is between parentheses). [g] $ee_{(S)\text{-}3g}$ (the value of $ee_{(S)\text{-}3a}$ is between parentheses). [h] $c_{(S)\text{-}3g}$ (conversion to (*S*)-**3g** + (*S*)-**3a** is between parentheses). [i] n.i.: not isolated.

Also after the continuous-flow DKR with *rac*-**2a**, this system was challenged with several benzylic amines having different steric and electronic properties to evaluate the substrate tolerance of the process (**Figure 14**.). The existence of functional groups which are reducible by transfer hydrogenation with the racemization catalyst, were the most obvious block of this type of DKR process. Exploratory experiments with 4-chloro-, 4-bromo- and 4-nitro-substituted phenylethan-1-amines revealed reduction of such groups under the racemization conditions leading those substances to be inappropriate with this type of DKR process.

Then, the DKR was investigated with six more valuable benzylic amines *rac*-**2b-g**. The KR process with a single *Ca*LB-TDP10-filled column (n= 1 for column A in **Figure 14**.) on *rac*-**2a-f** reported nearly 50% conversions. On the other hand, in case of bulkier amines *rac*-**2c** and *rac*-**2e** the single KR reactor gave mediocre conversions (n=1: 34% from *rac*-**2c** and 25% from *rac*-**2e**). For transformation of the aforementioned substrates, a two KR column system was applied (n= 2, column A in **Figure 14**.). It has been aimed to achieve conversion near to 50% in the KR part (column A) of the DKR systems.
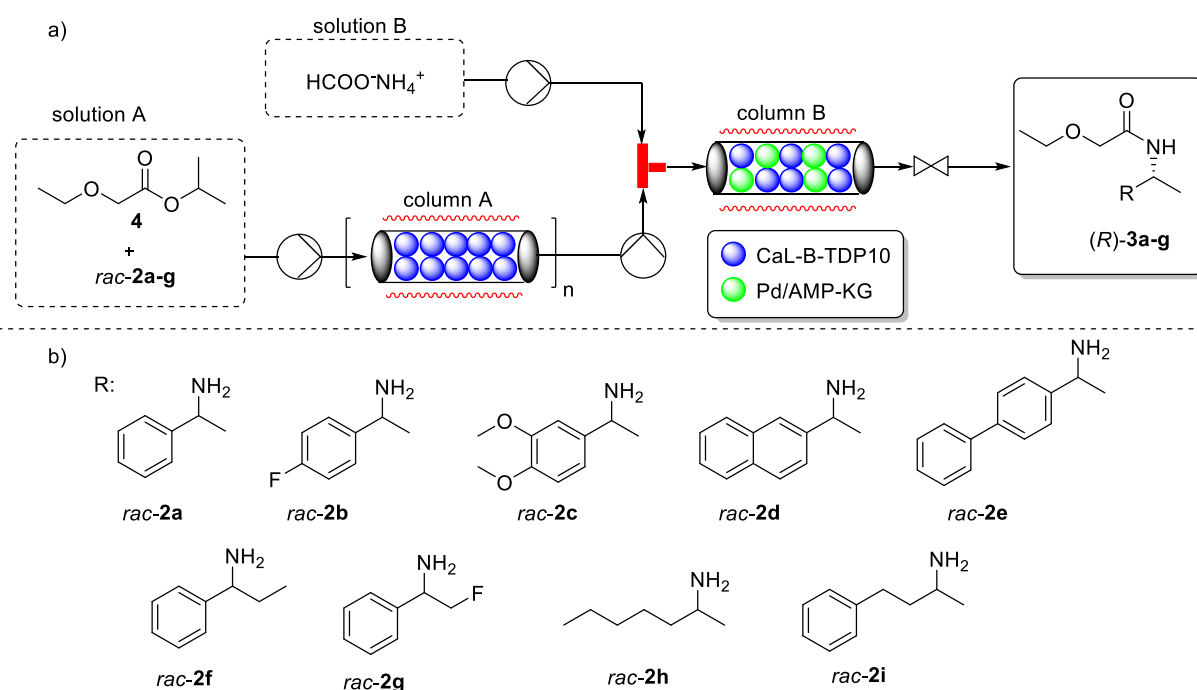
Figure 14. The constructed fully continuous system

The racemization performance could be deduced from the enantiomeric composition of the residual amine ($ee_{(S)\text{-}\mathbf{2a\text{-}g}}$). Effective racemization happened in the DKR of *rac*-**2a** (no **2a** remained, **Table 7**, entry 1), in the case of *rac*-**2d** ($ee_{(S)\text{-}\mathbf{2d}}$= 8.3%, **Table 7**, entry 4), respectively *rac*-**2f** ($ee_{(S)\text{-}\mathbf{2f}}$= 9.7%, **Table 7**, entry 6). Correspondingly, great to excellent conversions and yields were obtained in the DKR from these substrates (**Table 7**, entries 1,4,5). The slightly

pronounced positive inductive effect of the ethyl group attached to the benzylic position (*rac*-**2f**) did not inhibit racemization. In the case of *rac*-**2f**, the sparse conversion of DKR is a direct consequence of the decreased rate of the enzymatic KR, compared to the one observed with *rac*-**2a**.

Conceivably, in case of substrates with electron donating substituents, such as *rac*-**2c** (with 3,4-methoxy substituents) or *rac*-**2e** (with 4-phenyl substituent) the racemization was not performant ($ee_{(S)-2c}$= 63.3% and $ee_{(S)-2e}$= 74.4%; **Table 7.**, entries 3 and 5). Suddenly, the 4-fluoro substituent (*rac*-**2b**) had serious negative impact on racemization ($ee_{(S)-2b}$=92.0%, **Table 7.**, entry 2). The moderate efficiency of racemization, resulted only modest isolated yields (57-60%) however in the DKRs from *rac*-**2b,c,e** excellent enantiomeric purities (*ee* ≥98.9%) could be witnessed.

In DKR of *rac*-**2g** (a fluorine in an aliphatic position is present) it can be observed that the fluorine was partially reduced by the racemization agent under the selected DKR process conditions (0.6 equiv. of $HCOO^-NH_4^+$, 100 psi, 70 °C: **Table 7.**, entry 7). In this case as in the case before the enantiomeric purities of the fluorine containing product (*R*)-**3g** and of the dehalogenated byproduct (*R*)-**3a** were excellent ($ee_{(S)-2g}$ and $ee_{(S)-2g}$ >99%), nevertheless the enantiomeric composition of the residual halogenated substrate ($ee_{(S)-2g}$= 59%) showed medium efficiency of racemization for (*S*)-**2g**.

3.3.2. Operational stability

In general, under continuous-flow setup of a catalytic system its durability can be defined by its operational stability. Accordingly, the DKR system of *rac*-**2a** to (*R*)-**3a** was performed and supervised at 60 °C for 48 h concluding to excellent operational stability (**Figure 15.**). The constructed system was stable for at least 2 days, continuously producing enantiopure (*R*)-**3a** ($ee_{(S)-2a}$ >99.8%) with a space time yield of 103 kg m^{-3} day^{-1}.
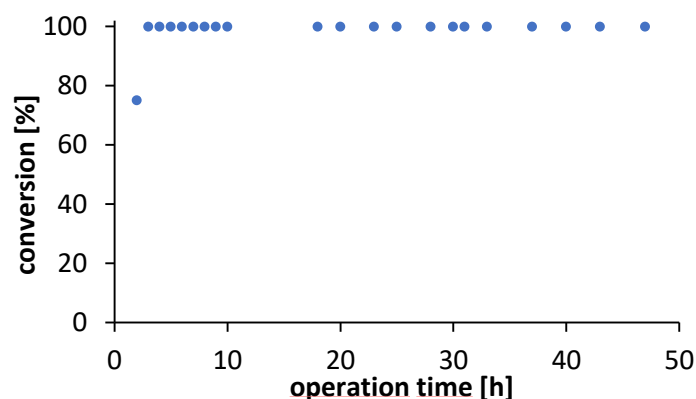
Figure 15. Operational stability of the Pd/AMP-KG–*Ca*LB-TDP10 DKR system (continuously operated) converting 1-phenyletan-1-amine (*rac*-**2a**) [GC conversion (●) is shown for the DKR system operated under conditions of **Table 7** for 48 h].

3.3.3. Conclusions

To conclude, the presented novel system, describes for the first time fully continuous-flow mode DKR of racemic benzylic amines (*rac*-**2a-f**). The dynamic kinetic resolution system implicated a robust lipase (*Ca*LB-TDP10) for kinetic resolution and a mild racemization agent with palladium on aminopropyl-grafted silica (Pd/AMP-KG). As hydrogen source ammonium formate was used, which fully dissolved in 2-methyl-2-butanol, thus could be utilized at reasonably high temperatures (60-70 ˚C). In this study, it has been highlighted that this racemization process was practical for benzylic amines which are not containing easily reducible functions. The developed DKR system contained: 1 or 2 packed-bed columns filled with *Ca*LB-TDP10 (KR unit) and a column filled with Pd/AMP-KG+*Ca*LB-TDP10 (mixed-bed dynamic kinetic resolution unit). These were applied favorably for the conversion of various valuable benzylic amines *rac*-**2a-f** to amides (*R*)-**3a-f** in medium to high isolated yields (57-96%) with excellent enantiomeric purities (>98.8%).

3.4. TAs in the kinetic resolution of amines

3.4.1. Identification of new TAs

The gene mining was performed on the NCBI (National Center for Biotechnological Information) for the (*S*)- or (*R*)-selective transaminases using the highly conserved motifs of: the (*S*)-selective TA from *Vibrio fluvialis* (F2XBU9, *Vf*-TA); *Chromobacterium violaceum* (Q7NWG4, *CvS*-TA); *Halolamina sediminis* (A0A1J0VCU3, *Hs*-TA) and *Halomonas elongata* (E1V913, *He*-TA) or the (*R*)-selective TA from *Capronia semiimmersa* TA (A0A0D2DZI3, *Cs*-TA); *Artrobacter sp*. (F7J696, *Ar*-TA) and *Thermomyces stellatus* TA (pdb: 6XWB_A, *Ts*-TA).

The amino acid sequence identity of the selected (*S*)-selective transaminases *Pseudomonas psychrotolerans* (*PpS*-TA) to *CvS*-TA, *Vf*-TA, *He*-TA and *Hs*-TA were 55.3%, 36.2%, 64.4% and 61.3% respectively, showing the most recent ancestor with *He*-TA and *Hs*-TA. The amino acid sequence identity of the selected (*R*)-selective transaminases from *Sinorhizobium* sp (*SrR*-TA) to *Cs*-TA, *Ar*-TA and *Ts*-TA is 40%, 54.9% and 62.2% respectively, revealing the most recent ancestor with *Ts*-TA

First it was tested whether the new TAs can accept *rac*-**7a-d** as their amino donors. It has been concluded that all tested amines were substrates for the newly discovered TAs (**Figure 16.**). One important aspect is that none of **6a-d** acted as amino acceptors for the aforementioned TAs, it was not possible to detect any (*S*)- or (*R*)-**7a-d** in the asymmetric synthesis pathway. Furthermore, they were incubated with 10 equiv. of (*S*)- or (*R*)-alanine and in this case as well no amine product was identified. This resulted in the possibility of supervision of the irreversible kinetic resolutions on chiral HPLC, highlighting in this way the opposite enantioselectivity of the freshly discovered TAs.
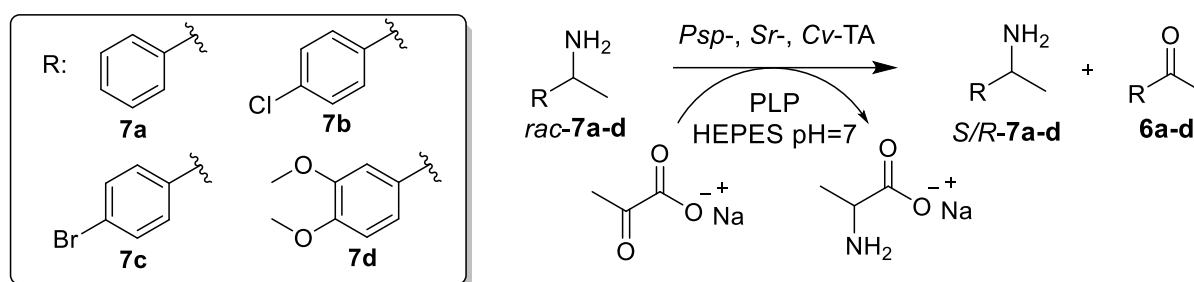
Figure 16. KR with TAs on *rac*-1-phenylethylamines and pyruvate (using purified enzymes of *PpS*-, *SrR*-, *CvS*-TA W60C variant)

3.4.2. Functional activity/stability tests

3.4.2.1. pH optimum for the new TAs

In the case of the (*S*)- and (*R*)-selective transaminases their activity was measured within the desired kinetic resolution mode (**Figure 16.**), with 1-phenylethylamine (*rac*-**7a**) as a model substrate, in the range of pH 6.2-12 by initial velocity-based activity tests. Thus, for the *PpS*-TA the highest relative activity was achieved in the pH range from 9 to 11, which is considerably wider pH range compared to other TAs[65 66 67 68 69]. For pH values >11.0 and < 8.0 decreased enzymatic activity was observed (**Figure 17a**). The thermal stability measurements revealed that the thermal stability of protein fold of the (*S*)-selective TA is reserved in a wide pH range from 6.5 to 9.5 (**Figure 17a**). At pH = 6.2 and at pH > 11.0 the structural stability of the enzyme drops, which is confirmed by the decreased melting temperatures (T_m) to 39.5 and 43.5 ˚C respectively (**Figure 17b**).
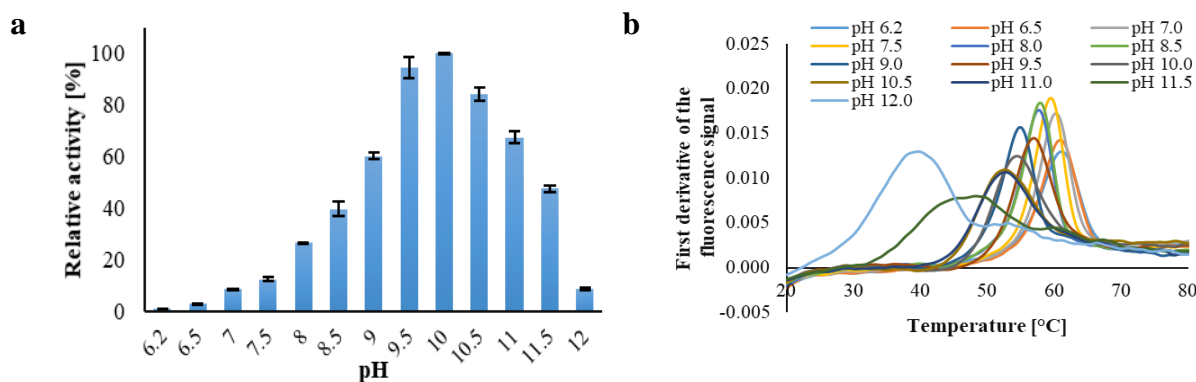
Figure 17. a) the pH effect on *PpS*-TA activity, **b)** thermal unfolding curves of *PpS*-TA

In the case of the (*R*)-selective TA, the investigations of the pH effect upon the enzymatic activity resulted a tighter pH range. The maximum activity was observed at pH 7.5 and for the pH values > 8.0 an activity drop was witnessed (**Figure 18a**). Differential thermal calorimetric measurements revealed that the *SrR*-TA has modest thermal stability, although at pH = 6 a T_m maximum of 49 ˚C was measured (**Figure 18b**).
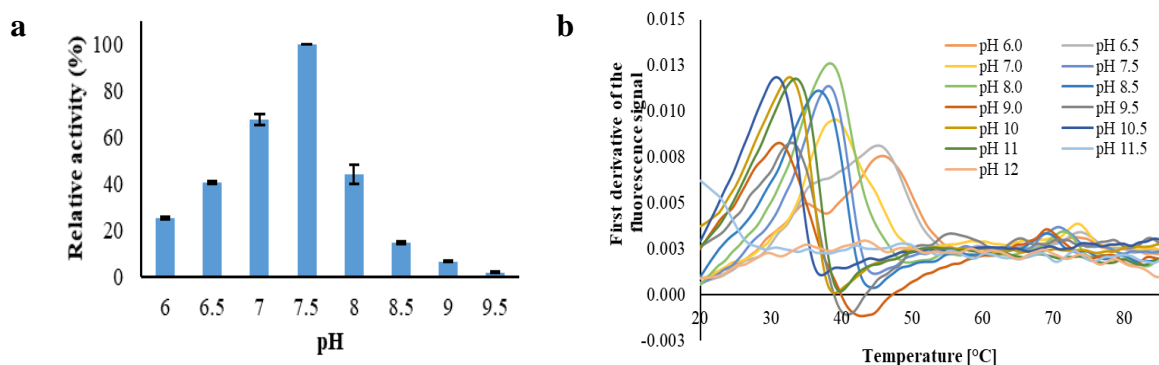
Figure 18. a) The pH effect on *SrR*-TA activity **b)** thermal unfolding curves of *SrR*-TA at different pH values

3.4.2.2. Buffer screening of the TA in kinetic resolution mode

In this set of screening to get to the optimal buffer system, the previously used kinetic resolution of *rac*-**7a** was applied in various buffer solutions (phosphate, HEPES, phosphate-saline – 50 and 100 mM) at the optimal pH=7 value. The biocatalytic reactions performed with *PpS*-TA in HEPES, resulted after 1 h reaction time nearly 50% conversion, in the case of *SrR*-TA 38% was obtained after 22 h reaction time in HEPES (**Figure 19.**). If PBS buffer was used, in 100 mM concentration, minimal conversion values were obtained for both biocatalysts. For further screenings HEPES in 50 mM concentration was used in both cases.
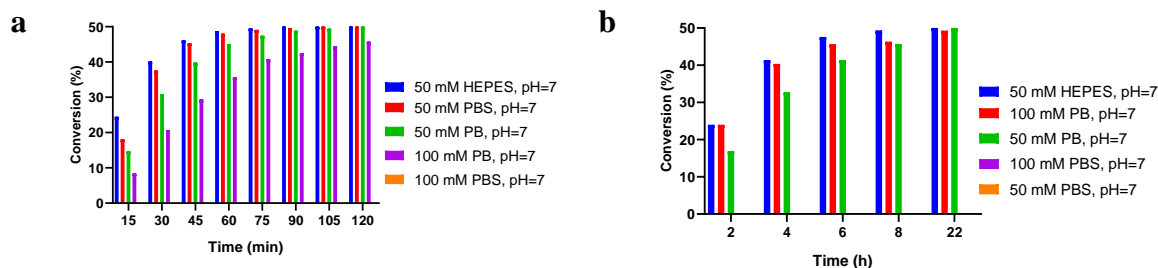
Figure 19. **a)** *PpS*-TA catalyzed KR, conversion in the function of time in various buffer systems at 40 ˚C; **b)** *SrR*-TA catalyzed KR, conversion in the function of time in various buffer systems at 25 ˚C

3.4.2.3. Thermal stability of the new biocatalysts

It was aimed to follow the conversion change in the KR setup of the model substrate *rac*-**7a** under the previously established conditions (50 mM pH=7 HEPES buffer) at various temperatures. In the case of *PpS*-TA the temperature range was 20-55 ˚C and for *SrR*-TA 20-40 ˚C in which the conversion was registered. In this screening our ambition was also to determine the operational stability in the conversion-based activity, in the case of incubation/operation (0, 1, 2, 3, 4, 5, 6, 7, 8 h and 22 h incubation) at previously set temperatures (**Figure 17b.** and **Figure 18b.**). This could reveal the operational robustness of the biocatalysts.

The conversions of the *PpS*-TA catalyzed reactions were increased with the increasing of the temperature in the range of 20-55 ˚C. Maximal conversion values were obtained after 0.5 h at 55 ˚C, which in the case of 45 ˚C and 50˚C was increased to 1 h reaction time. Beginning with 6 h pre-incubation of the biocatalyst at the previously mentioned temperatures, the TA maintained its conversion-based activity until 45 ˚C ($c_{45°C}$ = 49.3%), which was followed by a significant decrease of activity in comparison to the initial values. Lastly, the 22 h incubations showed a local maximum $c_{40°C}$ = 44.5% which is 5% lower in comparison to the non-incubated enzyme at the same temperature. These information highlights an operational stability in the range of 20-45 ˚C for the *PpS*-TA (**Figure 20.**).
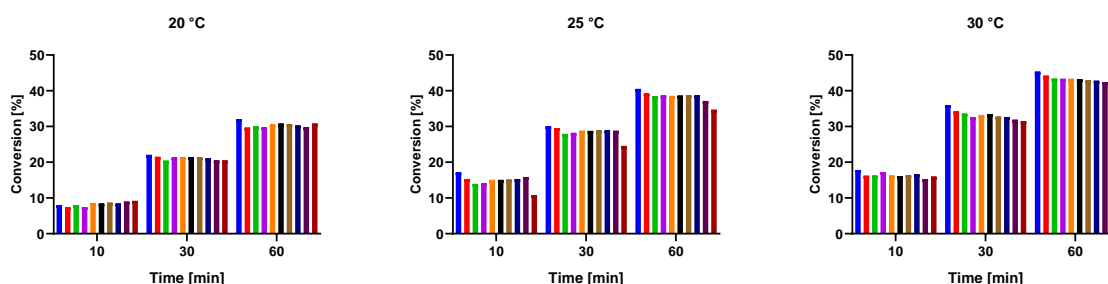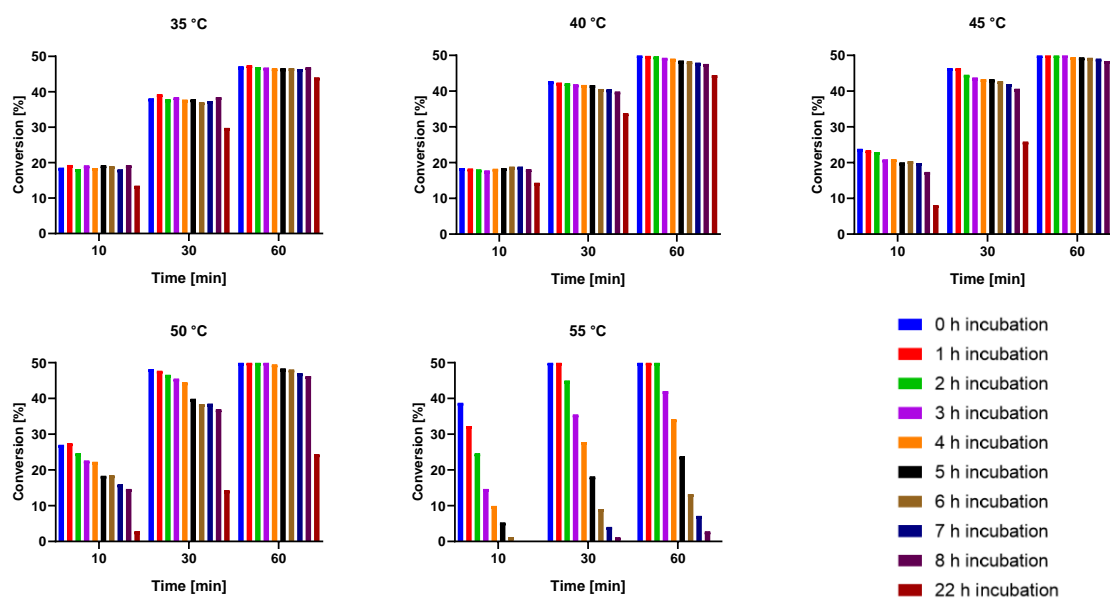
Figure 20. Temperature influence on *PpS*-TA activity (different pre-incubation time for the biocatalyst), using 10 mM *rac*-**7a** as substrate and 10 mM pyruvate as co-substrate, 1 h reaction time

Under the same kinetic resolution setup of *rac*-**7a**, first the *SrR*-TA was screened without pre-incubation of the enzyme. It was observed a decreasing tendency in the conversion-based activity, when the temperature was elevated from 20 to 40 °C ($c_{20°C}$ = 21.7% and $c_{40°C}$ = 10.4%), half of the activity was lost in the 1 h screening. In the case of the 6 h pre-incubation of the TA the 20-35 °C temperatures did not lead to negative impact on activity, however higher temperatures caused significant activity loss related to the non-incubated one at the same temperature over the established reaction time. Meanwhile the 22 h pre-incubation yielded a 5-fold activity loss to non-incubated at 40 °C ($c_{40°C}$ = 2.2%) and a 10-fold activity decrease to the non-incubated at 20 °C ($c_{20°C}$ = 21.8%) in the 1 h screening (**Figure 21.**). The obtained results indicated decreased thermal stability for the (*R*)-selective *SrR*-TA, which is comparable to other (*R*)-selective TAs, although successful projects were reported in order to tackle this problematic.[70][71][72]
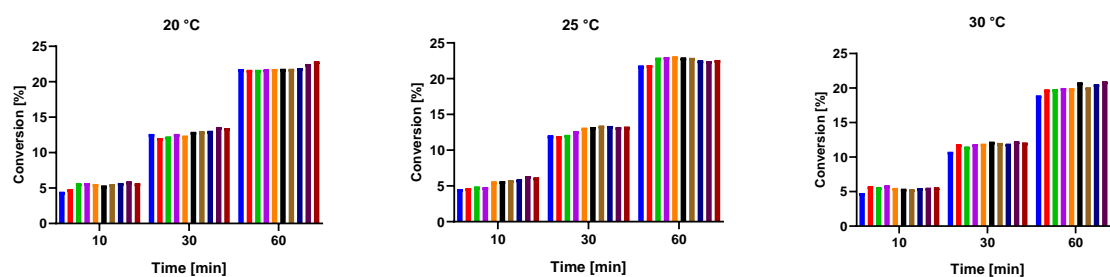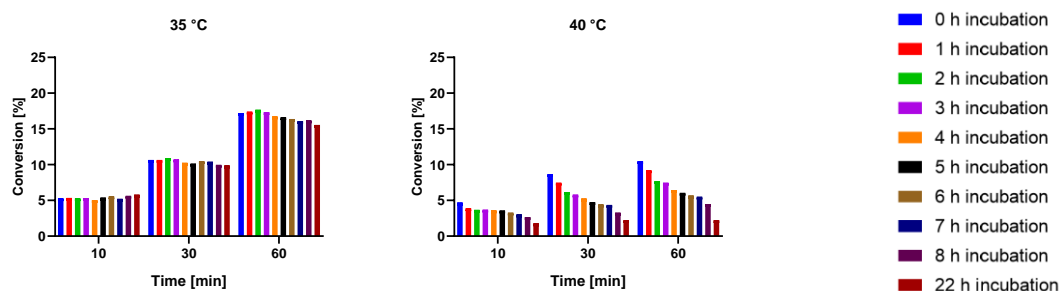
Figure 21. Temperature influence on *SrR*-TA activity (different pre-incubation time for the biocatalyst), using 10 mM *rac*-**7a** as substrate and 10 mM pyruvate as co-substrate, 1 h reaction time

3.4.2.4. Influence of the co-solvent on the stability/activity of the novel TAs

Additionally, it was investigated the DMSO effect upon the conversion-based activity screening of the TAs on *rac*-**7a**. The (*S*)-selective TA without pre-incubation with DMSO, performed as it has been expected until 30% DMSO (v/v) content, which can be translated as full conversion after 1 h (under the previously described screening conditions). If the *PpS*-TA is incubated for 1-8 h with different DMSO amounts, 25% (v/v) is the topmost amount with which full conversion values can be obtained. The increasing DMSO amounts caused big decreases in enzyme activity, reflected in minimal conversion values (**Figure 22.**).
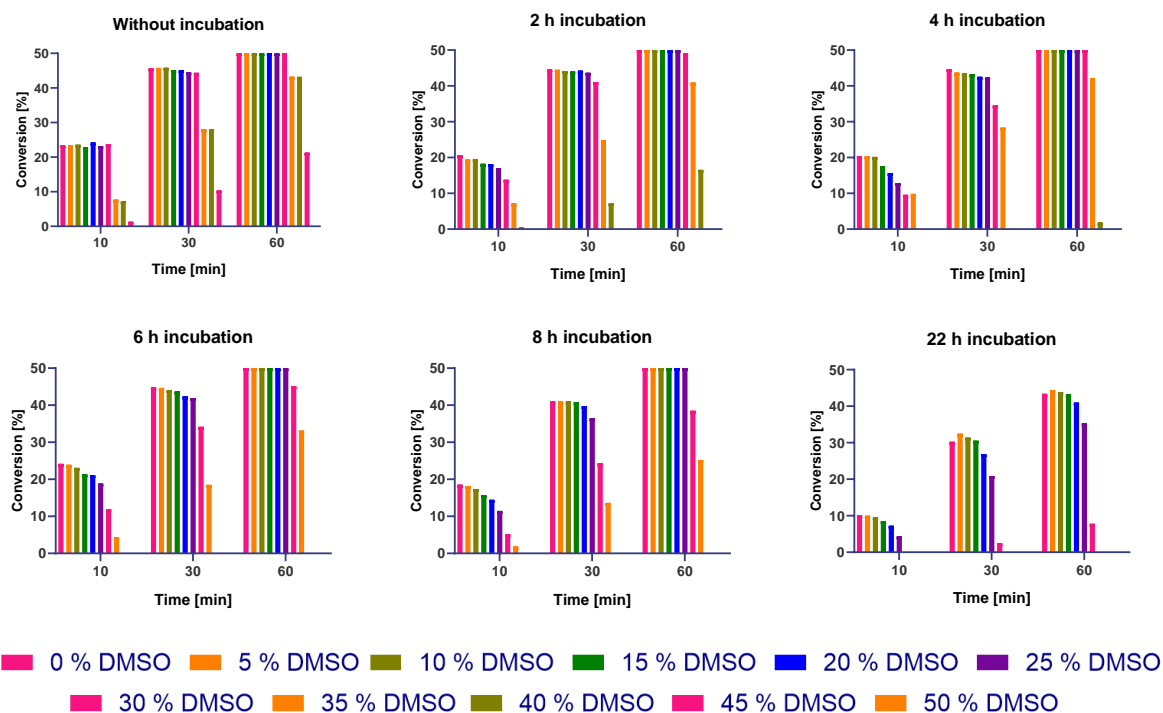
Figure 22. The *PpS*-TA conversion-based activity profile of *rac*-**7a** with different DMSO contents and various incubation times

34

The (*R*)-selective TA, without prior incubation, produced similar conversions until 20% DMSO content which in case of higher co-solvent values was followed by conversion drop. Longer incubation did not cause deficit in activity, even in the case of 22 h incubation with 20% DMSO, the conversion was 20% after 1 h reaction time, which was the same value for the not incubated enzyme (**Figure 23.**).
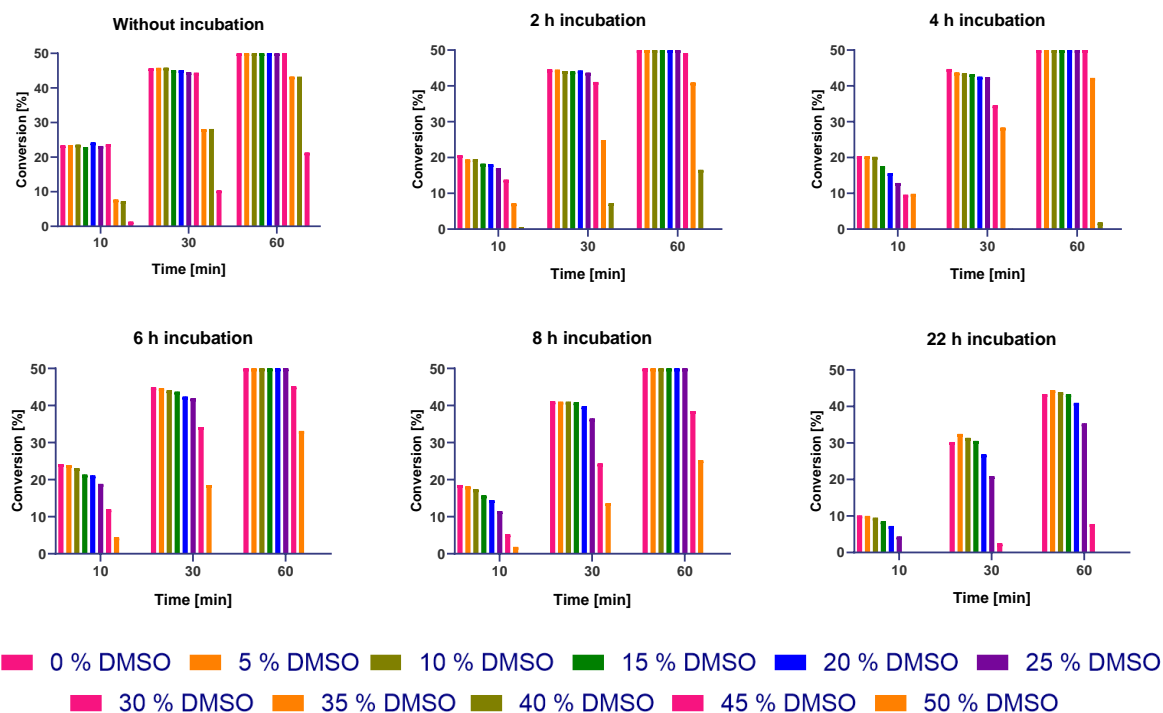
Figure 23. The *SrR*-TA conversion-based activity profile of *rac*-**7a** with different DMSO contents and various incubation times

3.4.2.5. Kinetic characterization of the novel biocatalysts

It was also desired to determine the catalytic efficiency of the novel TAs. To achieve this goal kinetic measurements were planned on various racemic amines (*rac*-**7a, -7b, -7c, -7d**) and pyruvate (co-substrate). The resulting data was compared to the well-studied W60C variant of the TA from *Chromobacterium violaceum* (*CvS*-TA)[73][74][75]. Initially, the kinetic parameters were determined for *PpS*-TA and *SrR*-TA, at fixed (0.6 mM) pyruvate concentration for the above mentioned substrates (**Figure 16.**, **Table 10**).

Overall, with all substrates (except in the case of transamination of *SrR*-TA with *rac*-**7b**) the *SrR*-, and *PpS*-TA have higher K_M values than *CvS*-TA W60C variant (*CvS*-TA), which values are suggesting lower substrate affinity. These results however, can be connected to the elevated v_{max} and k_{cat} values, which point out that the new TAs are more efficient at higher substrate concentrations than the *CvS*-TA (**Table 10**). In **Table 10** can be witnessed a ~12-fold

increased catalytic efficiency for *PpS*-TA and ~2.5 fold increased values for *SrR*-TA (represented by k_{cat} values in both cases) for the *rac*-**7a** in relation with *CvS*-TA. Surprisingly this was linked with a relaxed orientation of the substrate (*rac*-**7a**) which can be deduced from the increased K_M values (14-fold increase for *PpS*-TA and 16.5-fold increase for *SrR*-TA) related to *CvS*-TA. Looking at the case of *rac*-**7b**, K_M and k_{cat} values of comparable degree were obtained for the three TAs. In case of *rac*-**7c,d** *PpS*-TA was the most active, showing ~9-fold higher catalytic efficiency (k_{cat}) joined with a ~23-fold increased K_M values in comparison to W60C variant of *CvS*-TA.

The *SrR*-TA shows truly lower (311.7 and 37.6-fold) k_{cat} value in the transamination of *rac*-**7a** than those measured for other (*R*)-selective TAs *Fusarium oxysporum*-TA[76] and *Aspergillus terreus* TA correspondingly. This highlights low catalytic efficiency for *SrR*-TA, but diverse assay conditions may influence the data. Furthermore, related to the enhanced variant of *CvS*-TA slightly increased k_{cat} values (for *rac*-**7a,c**) or analogous (for *rac*-**7b,d**) are witnessed in **Table 10**, which results are confirming its biocatalytic potential.

Table 10. Kinetic data for the *PpS*-TA and *SrR*-TA compared with *CvS*-TA (W60C) by *rac*-**7a-d** as substrates.

	PpS-TA			*SrR*-TA			*CvS*-TA (W60C)		
	K_M [µM]	v_{max} [µM/s]	k_{cat} [s⁻¹]	K_M [µM]	v_{max} [µM/s]	k_{cat} [s⁻¹]	K_M [µM]	v_{max} [µM/s]	k_{cat} [s⁻¹]
rac-**7a**	448	0.212	0.085	531	0.047	0.017	32	0.014	0.007
rac-**7b**	161	0.041	0.016	126	0.058	0.021	128	0.028	0.014
rac-**7c**	952	0.541	0.217	341	0.237	0.085	40	0.047	0.024
rac-**7d**	899	0.453	0.182	175	0.057	0.020	38	0.044	0.022

Kinetic parameters represent the apparent rate constants determined at a fixed concentration of pyruvate (0.6 mM).

This was followed by determining the kinetic data of the novel TAs by fixing the *rac*-**7b** concentration (0.6 mM) and altering the pyruvate amount in the reactions (**Table 11**). Notably, in the kinetic measurements of *rac*-**7b**, the high k_{cat} values also approve the high catalytic efficiency of the novel TAs. The turnover number of pyruvate (**Table 11**) are in all cases superior to the ones obtained for the screening of *rac*-**7a-d** (**Table 10**) on *CvS*-TA W60C. In the case of pyruvate kinetics, the investigated variant of *CvS*-TA showed higher affinity for *rac*-**7b** (K_M = 128 µM – **Table 10**), like the one showed for pyruvate (K_M = 399 µM – **Table 11**). *PpS*-TA performed the other way around, with high affinity for pyruvate (K_M = 43 µM – **Table 11**) and low affinity (K_M = 161 µM – **Table 10**) towards *rac*-**7b**. The *SrR*-TA performed alike in these two comparison (**Table 10,11**).

Table 11. Kinetic data for the *PpS*-TA and *SrR*-TA compared
with W60C *CvS*-TA with pyruvate.

	pyruvate		
	K_M [µM]	v_{max} [µM/s]	k_{cat} [s^{-1}]
PpS-TA	43	0.195	0.078
SrR-TA	121	0.202	0.072
CvS-TA (W60C)	399	0.067	0.034

Kinetic parameters represent the apparent rate constants determined at a
fixed concentration of *rac*-**7b** (0.6 mM).

3.4.2.5.1. Substrate inhibition determination

In the kinetic measurements, the determined curves have suggested a minor substrate inhibition in the case of *CvS*-TA on *rac*-**7a** which has not been detected in the case of *PpS*- and *SrR*-TA (**Figure 24.**).
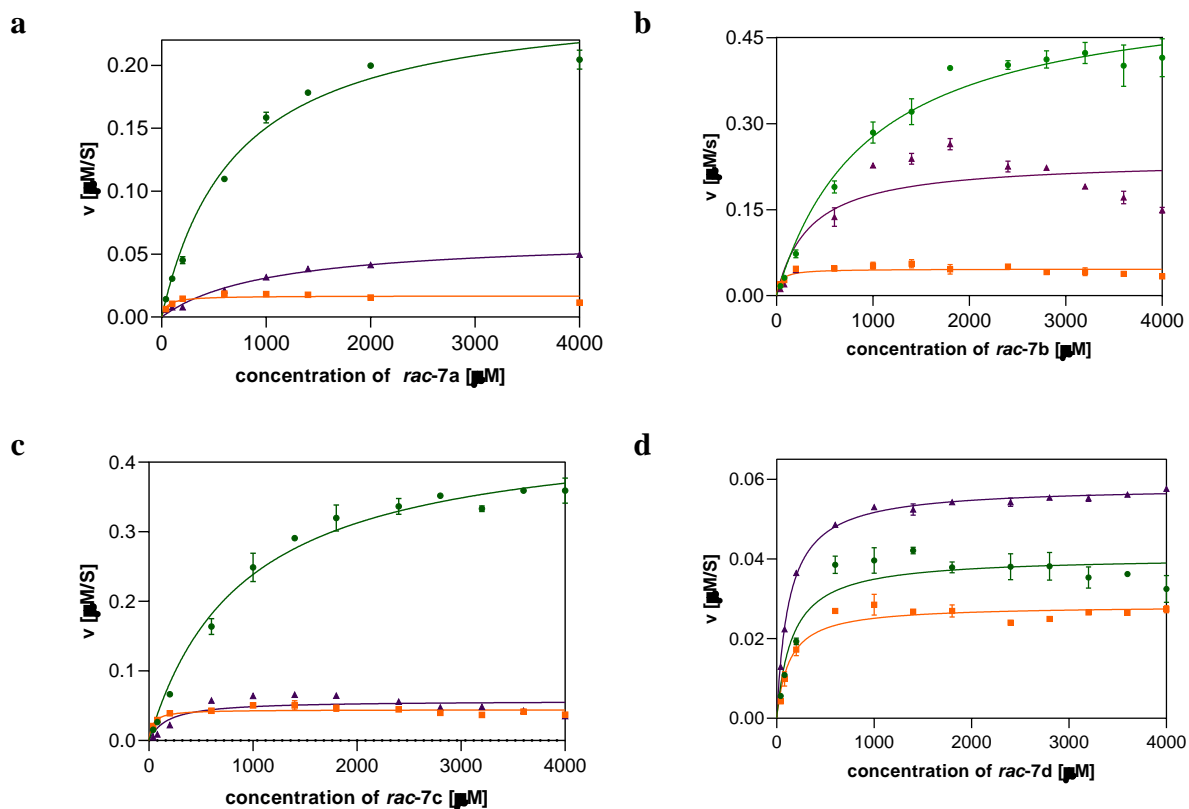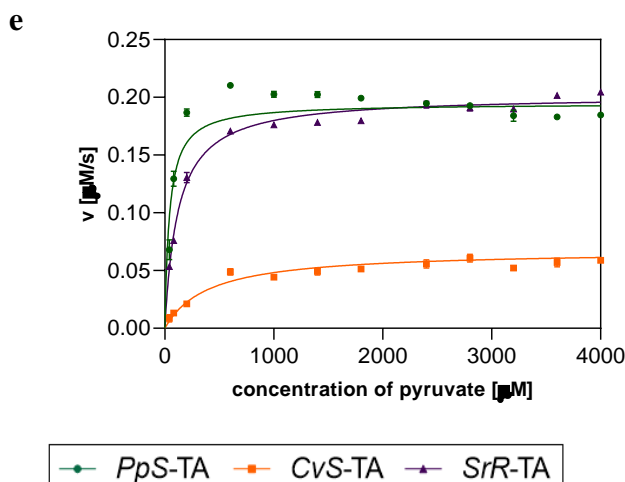
Figure 24. Substrate inhibition measurement for *rac*-**7a-d** and pyruvate

For *rac*-**7b,c** medium substrate inhibition was observed if *SrR*-TA was used, however this was not the case for *PpS*- and *CvS*-TA (**Figure 24b,c**). Minor substrate inhibition was observed in the *PpS*-TA driven transamination of *rac*-**7d** (**Figure 24d.**). Investigations were performed from the pyruvate (amino acceptor) site as well, where moderate inhibition can be observed in the case of *PpS*-TA. For this biocatalyst the removal of the pyruvate from the reaction media may be an important factor to consider, in order to get the optimal catalytic performance while using it. The *SrR*- and *CvS*-TAs were not hindered by increasing concentrations of pyruvate (**Figure 24e.**).

3.4.2.5.2. Product inhibition measurements

For this set of experiments, it was desired to check the inhibitory effect of the ketone generated from the KR, because it is known that these substances can act as inhibitors[77] for the reaction. Thus, the UV-assay was used to check whether product inhibition is present using the *rac*-**7a-d** amines as substrates. The formed acetophenones were better inhibitors for all investigated TAs than the substrates (**Figure 25a-d**). In the case of *CvS*-TA and *SrR*-TA the acetophenone, **6a**, caused severe inhibition even at 0.3 mM concentration, at which their activity were reduced by 68% and 86%. The *PpS*-TA performed at ~50% under the same conditions with **6a** (**Figure 25a**).

The literature known *CvS*-TA showed significant product inhibition with all investigated acetophenones, with residual activity of 59% at 0.5 mM of **6b** (**Figure 25b**), 36% at at 0.5 mM of **6c** (**Figure 25c**) and lastly 30% at 0.5 mM of **6d** (**Figure 25d**).

In the screenings performed with *SrR*-TA, the **6b** and **6c** ketones caused moderate inhibition, the initial activity was decreased to 45% at 0.6 mM ketone concentrations of the aforementioned ketones (**Figure 25b,c**). However, in the concentration range tested for **6d**, 10% of activity loss was observed for the (*R*)-selective TA (**Figure 25d**), higher concentrations could not be tested due to the limitations of the given assay conditions.

The *PpS*-TA was inhibited mostly by **6c**, ~33% remaining activity at 0.6 mM of **6c** (**Figure 25c**), at the same time in the case of **6d** ~50% of the initial activity was lost (**Figure 25d**). In the case of **6b** minor impact was observed, ~75% residual activity registered at 0.5 mM concentration of **6b** (**Figure 25b**).
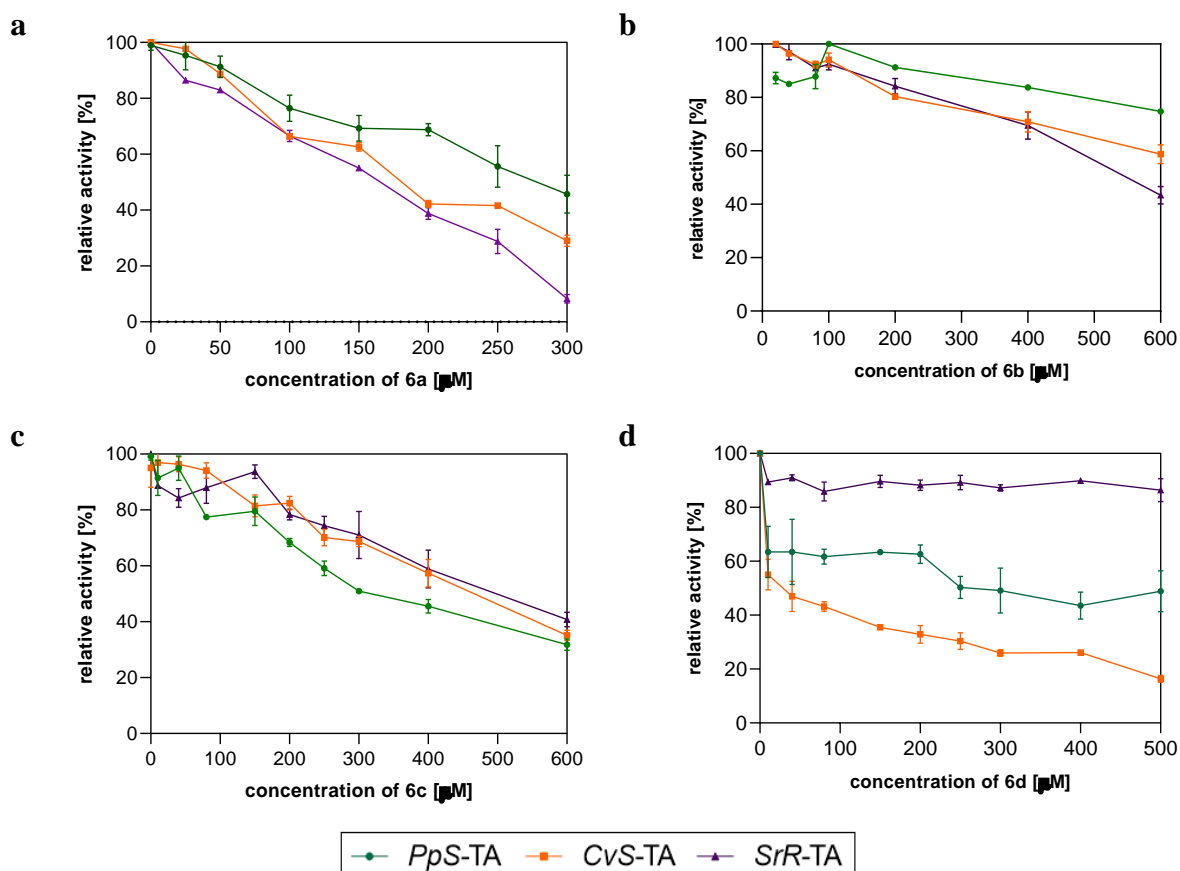
Figure 25. Product inhibition of the tested TAs at various ketone concentrations of a) **6a**, b) **6b**, c) **6c**, d) **6d**

3.4.3. Conclusions

Using the tools of gene mining for (*R*)- and (*S*)-selective transaminases, using conserved sequence motifs of their PLP binding sites, *Shinorizobium* sp. TA (*SrR*-TA) and *Pseudomonas psychrotolerans* TA (*PpS*-TA) were selected. The operational stabilities of the

transaminases however showed that pH=7 is the best for the conversion-based determination of the activities of *rac*-**7a**.

In the operational stability as a function of temperature in the transaminations, it has been revealed that for the *PpS*-TA 22 h pre-incubation lead to complete activity loss, however at 40 ˚C only just 5% conversion decrease was observed between the non-incubated biocatalyst and the one which has been incubated for 22 h prior test reaction. The *SrR*-TA has its operational peak at 35 ˚C and unfortunately, at 40 ˚C and 22 h pre-incubation 5-fold activity loss has been witnessed.

Incubation of the (*S*)-selective enzyme with DMSO resulted low long term stability of the TA, for 22 h incubation within the mentioned co-solvent amount of 5-50% DMSO (v/v), worse conversion values were obtained as without DMSO. For the (*R*)-selective TA the obtained conversion values have not had a negative impact even by 35% DMSO (v/v) content. Surprisingly, in the case of 22 h incubation with 35% DMSO, this helped the enzyme obtaining higher conversion values in comparison to the one registered without incubation with the same amount co-solvent.

The kinetic measurements revealed that the novel (*S*)-selective *PpS*-TA in the kinetic resolution of the studied *rac*-**7a**-**d** amines outpaced in terms of catalytic efficiency, represented by turnover number (k_{cat}), the well-characterized W60C variant of *CvS*-TA. From substrate and product inhibition measurements it became clear that improved tolerance towards substrate concentration is represented by the TAs. Nonetheless, **6a** powerfully inhibits all enzymes, while for **6b**-**d** medium inhibition was measured for *SrR*- and *CvS*-TA, yet *PpS*-TA being less sensible for the elevated concentrations of **6b**-**d**.

Generally, these results presenting the two novel TAs as prosperous biocatalysts, with high operational stability for the production of enantiomerically enriched amines.

4. General conclusions

In this study, it has been aimed to offer new procedures (through novel enzymes or via new setups) for the optically pure production of amines and alcohols.

First, a stable, robust and active immobilization procedure was developed for the CaL-B, which enabled the production of the optically pure secondary alcohols on a hundred-gram scale. The obtained dataset highlighted the practicability of the biocatalyst in both batch and flow modus. This paved the way also for a fast optimization and easy handling of the catalyst. Using this method, demonstrated on various substrates, excellent enantioselectivity values were obtained in kinetic resolutions, which poses favorably this work for multi-gram scale synthesis of secondary alcohols.

Second, to develop a fully-continuous dynamic kinetic resolution setup of various optically active amines, CaL-B enzyme and a racemization catalyst (palladium on aminopropyl-silica) was used. In this work, it has been demonstrated how helpful may be the serial linking of racemization columns in order to obtain the maximum potential of the system. This stable system was used successfully on various amines with excellent enantioselectivities and yields.

Last but not least, two novel TAs were characterized. They are acting with excellent enantioselectivities in the kinetic resolution setup on the tested racemic amines. Determining their kinetic parameters and their operational limits have helped exploring the catalysts performance. The (*S*)-selective TA (*PpS*-TA) made impressive results in direct kinetic comparison with the well characterized W60C variant of *Chromobacterium violaceum* TA. The co-solvent tolerance of the (*R*)-selective TA (*SrR*-TA), is a reasonable ability which might be pushed further. Their properties are remarkable, thus they position them positively for further investigations.

5. References

[1] Tucker, J.L. and Faul, M.M., 2016. Industrial research: Drug companies must adopt green chemistry. *Nature News*, *534*(7605), p.27-29.

[2] Zaks, A. and Klibanov, A.M., 1984. Enzymatic catalysis in organic media at 100 degrees C. *Science*, *224*(4654), pp.1249-1251.

[3] Wender, P., 1997. Towards the ideal synthesis. *Chemistry and Industry*, (19), p.765-769.

[4] Bruggink, A., Schoevaart, R. and Kieboom, T., 2003. Concepts of nature in organic synthesis: cascade catalysis and multistep conversions in concert. *Organic process research & development*, *7*(5), pp.622-640.

[5] Abu, R. and Woodley, J.M., 2015. Application of enzyme coupling reactions to shift thermodynamically limited biocatalytic reactions. *ChemCatChem*, *7*(19), pp.3094-3105.

[6] Sheldon, R.A. and Brady, D., 2019. Broadening the scope of biocatalysis in sustainable organic synthesis. *ChemSusChem*, *12*(13), pp.2859-2881.

[7] Aslan, S., Noor, E. and Bar-Even, A., 2017. Holistic bioengineering: rewiring central metabolism for enhanced bioproduction. *Biochemical Journal*, *474*(23), pp.3935-3950.

[8] Bryan, M.C., Dunn, P.J., Entwistle, D., Gallou, F., Koenig, S.G., Hayler, J.D., Hickey, M.R., Hughes, S., Kopach, M.E., Moine, G. and Richardson, P., 2018. Key Green Chemistry research areas from a pharmaceutical manufacturers' perspective revisited. *Green Chemistry*, *20*(22), pp.5082-5103.

[9] Sheldon, R.A., Brady, D. and Bode, M.L., 2020. The Hitchhiker's guide to biocatalysis: recent advances in the use of enzymes in organic synthesis. *Chemical science*, *11*(10), pp.2587-2605.

[10] Plutschack, M.B., Pieber, B., Gilmore, K. and Seeberger, P.H., 2017. The hitchhiker's guide to flow chemistry‖. *Chemical reviews*, *117*(18), pp.11796-11893.

[11] Gutmann, B., Cantillo, D. and Kappe, C.O., 2015. Continuous-flow technology—a tool for the safe manufacturing of active pharmaceutical ingredients. *Angewandte Chemie International Edition*, *54*(23), pp.6688-6728.

[12] Martin, L.L., Peschke, T., Venturoni, F. and Mostarda, S., 2020. Pharmaceutical industry perspectives on flow chemocatalysis and biocatalysis. *Current Opinion in Green and Sustainable Chemistry*, *25*, p.100350.

[13] Santi, M., Sancineto, L., Nascimento, V., Braun Azeredo, J., Orozco, E.V., Andrade, L.H., Gröger, H. and Santi, C., 2021. Flow biocatalysis: a challenging alternative for the synthesis of APIs and natural compounds. *International journal of molecular sciences*, *22*(3), p.990.

[14] Thompson, M.P., Peñafiel, I., Cosgrove, S.C. and Turner, N.J., 2018. Biocatalysis using immobilized enzymes in continuous flow for the synthesis of fine chemicals. *Organic Process Research & Development*, *23*(1), pp.9-18.

[15] De Vitis, V., Dall'Oglio, F., Tentori, F., Contente, M.L., Romano, D., Brenna, E., Tamborini, L. and Molinari, F., 2019. Bioprocess intensification using flow reactors: Stereoselective oxidation of achiral 1, 3-diols with immobilized Acetobacter aceti. *Catalysts*, *9*(3), p.208.

[16] Heider, P.L., Born, S.C., Basak, S., Benyahia, B., Lakerveld, R., Zhang, H., Hogan, R., Buchbinder, L., Wolfe, A., Mascia, S. and Evans, J.M., 2014. Development of a multi-step synthesis and workup sequence for an integrated, continuous manufacturing process of a pharmaceutical. *Organic Process Research & Development*, *18*(3), pp.402-409.

[17] Thomas, C.R. and Geer, D., 2011. Effects of shear on proteins in solution. *Biotechnology letters*, *33*(3), pp.443-456.

[18] Britton, J., Majumdar, S. and Weiss, G.A., 2018. Continuous flow biocatalysis. *Chemical Society Reviews*, *47*(15), pp.5891-5918.

[19] Schweidtmann, A.M., Clayton, A.D., Holmes, N., Bradford, E., Bourne, R.A. and Lapkin, A.A., 2018. Machine learning meets continuous flow chemistry: Automated optimization towards the Pareto front of multiple objectives. *Chemical Engineering Journal*, *352*, pp.277-282.

[20] Zhu, Y., Chen, Q., Shao, L., Jia, Y. and Zhang, X., 2020. Microfluidic immobilized enzyme reactors for continuous biocatalysis. *Reaction Chemistry & Engineering*, *5*(1), pp.9-32.

[21] Mattey, A.P., Citoler, J., Baldwin, C., Marshall, J., Pamer, R., Turner, N., Cosgrove, S. and Flitsch, S., 2021. Production of high value amine intermediates via biocatalytic cascades in continuous flow.

[22] Summary of the Pollution Prevention Act. http://www.epa.gov/laws-regulations/summary-pollution-prevention-act (accessed on 05.10.2021)

[23] De Camp, W.H., 1989. The FDA perspective on the development of stereoisomers. *Chirality*, *1*(1), pp.2-6.

[24] Verho, O. and Bäckvall, J.E., 2015. Chemoenzymatic dynamic kinetic resolution: a powerful tool for the preparation of enantiomerically pure alcohols and amines. *Journal of the American Chemical Society*, *137*(12), pp.3996-4009.

[25] Tan, Z., Ma, H., Li, Q., Pu, L., Cao, Y., Qu, X., Zhu, C. and Ying, H., 2016. Biosynthesis of optically pure chiral alcohols by a substrate coupled and biphasic system with a short-chain dehydrogenase from Streptomyces griseus. *Enzyme and microbial technology*, *93*, pp.191-199.

[26] Hiraishi, T. and Taguchi, S., 2009. Enzyme-catalyzed synthesis and degradation of biopolymers. *Mini-Reviews in Organic Chemistry*, *6*(1), pp.44-54.

[27] Patel, R.N., 2011. Biocatalysis: Synthesis of key intermediates for development of pharmaceuticals. *Acs Catalysis*, *1*(9), pp.1056-1074.

[28] Liu, H., De Souza, F.Z.R., Liu, L. and Chen, B.S., 2018. Immobilized and free cells of Geotrichum candidum for asymmetric reduction of ketones: stability and recyclability. *Molecules*, *23*(9), p.2144.

[29] Faber, K., 2018. Introduction and background information. In *Biotransformations in organic chemistry* (pp. 1-30). Springer, Cham.

[30] Resch, V. and Hanefeld, U., 2015. The selective addition of water. *Catalysis Science & Technology*, *5*(3), pp.1385-1399.

[31] Yamashita, Y., Yasukawa, T., Yoo, W.J., Kitanosono, T. and Kobayashi, S., 2018. Catalytic enantioselective aldol reactions. *Chemical Society Reviews*, *47*(12), pp.4388-4480.

[32] Bracco, P., Busch, H., von Langermann, J. and Hanefeld, U., 2016. Enantioselective synthesis of cyanohydrins catalysed by hydroxynitrile lyases–a review. *Organic & biomolecular chemistry*, *14*(27), pp.6375-6389.

[33] Nealon, C.M., Musa, M.M., Patel, J.M. and Phillips, R.S., 2015. Controlling substrate specificity and stereospecificity of alcohol dehydrogenases. ACS Catal 5 (4): 2100–2114.

[34] Adlercreutz, P., 2013. Immobilisation and application of lipases in organic media. *Chemical Society Reviews*, *42*(15), pp.6406-6436.

[35] Steinreiber, A. and Faber, K., 2001. Microbial epoxide hydrolases for preparative biotransformations. *Current opinion in Biotechnology*, *12*(6), pp.552-558.

[36] Klein, C. and Hüttel, W., 2011. A Simple Procedure for Selective Hydroxylation of L-Proline and L-Pipecolic Acid with Recombinantly Expressed Proline Hydroxylases. *Advanced Synthesis & Catalysis*, *353*(8), pp.1375-1383.

[37] Chen, X.H., Wang, X.T., Lou, W.Y., Li, Y., Wu, H., Zong, M.H., Smith, T.J. and Chen, X.D., 2012. Immobilization of Acetobacter sp. CCTCC M209061 for efficient asymmetric reduction of ketones and biocatalyst recycling. *Microbial cell factories*, *11*(1), pp.1-14.

[38] Kazlauskas, R.J., Weissfloch, A.N., Rappaport, A.T. and Cuccia, L.A., 1991. A rule to predict which enantiomer of a secondary alcohol reacts faster in reactions catalyzed by cholesterol esterase, lipase from Pseudomonas cepacia, and lipase from Candida rugosa. *The Journal of Organic Chemistry*, *56*(8), pp.2656-2665.

[39] Höhne, M. and Bornscheuer, U.T., 2009. Biocatalytic routes to optically active amines. *ChemCatChem*, *1*(1), pp.42-51.

[40] Gotor-Fernández, V., Fernández-Torres, P. and Gotor, V., 2006. Chemoenzymatic preparation of optically active secondary amines: a new efficient route to enantiomerically pure indolines. *Tetrahedron: Asymmetry*, *17*(17), pp.2558-2564.

[41] Oláh, M., Boros, Z., Hornyánszky, G. and Poppe, L., 2016. Isopropyl 2-ethoxyacetate—an efficient acylating agent for lipase-catalyzed kinetic resolution of amines in batch and continuous-flow modes. *Tetrahedron*, *72*(46), pp.7249-7255.

[42] Pilissão, C., de Oliveira Carvalho, P. and da Graça Nascimento, M., 2009. Enantioselective acylation of (RS)-phenylethylamine catalysed by lipases. *Process Biochemistry*, *44*(12), pp.1352-1357.

[43] Päiviö, M., Perkiö, P. and Kanerva, L.T., 2012. Solvent-free kinetic resolution of primary amines catalyzed by Candida antarctica lipase B: effect of immobilization and recycling stability. *Tetrahedron: Asymmetry*, *23*(3-4), pp.230-236.

[44] Ghislieri, D. and Turner, N.J., 2014. Biocatalytic approaches to the synthesis of enantiomerically pure chiral amines. *Topics in Catalysis*, *57*(5), pp.284-300.

[45] Breuer, M., Ditrich, K., Habicher, T., Hauer, B., Keßeler, M., Stürmer, R. and Zelinski, T., 2004. Industrial methods for the production of optically active intermediates. *Angewandte Chemie International Edition*, *43*(7), pp.788-824.

[46] Busto, E., Gotor-Fernández, V. and Gotor, V., 2011. Hydrolases in the stereoselective synthesis of N-heterocyclic amines and amino acid derivatives. *Chemical reviews*, *111*(7), pp.3998-4035.

[47] Kroutil, W., Fischereder, E.M., Fuchs, C.S., Lechner, H., Mutti, F.G., Pressnitz, D., Rajagopalan, A., Sattler, J.H., Simon, R.C. and Siirola, E., 2013. Asymmetric preparation of prim-, sec-, and tert-amines employing selected biocatalysts. *Organic process research & development*, *17*(5), pp.751-759.

[48] Mourelle-Insua, Á., Méndez-Sánchez, D., Galman, J.L., Slabu, I., Turner, N.J., Gotor-Fernández, V. and Lavandera, I., 2019. Efficient synthesis of α-alkyl-β-amino amides by transaminase-mediated dynamic kinetic resolutions. *Catalysis Science & Technology*, *9*(15), pp.4083-4090.

[49] Guan, C., Ribeiro, A., Akkermans, A.D., Jing, Y., van Kammen, A., Bisseling, T. and Pawlowski, K., 1996. Nitrogen metabolism in actinorhizal nodules of Alnus glutinosa: expression of glutamine synthetase and acetylornithine transaminase. *Plant molecular biology*, *32*(6), pp.1177-1184.

[50] de la Torre, F., Santis, L.D., Suárez, M.F., Crespillo, R. and Cánovas, F.M., 2006. Identification and functional analysis of a prokaryotic-type aspartate aminotransferase: implications for plant amino acid metabolism. *The Plant Journal*, *46*(3), pp.414-425.

[51] Kohls, H., Steffen-Munsberg, F. and Höhne, M., 2014. Recent achievements in developing the biocatalytic toolbox for chiral amine synthesis. *Current opinion in chemical biology*, *19*, pp.180-192.

[52] Simon, R.C., Richter, N., Busto, E. and Kroutil, W., 2014. Recent developments of cascade reactions involving ω-transaminases. *ACS catalysis*, *4*(1), pp.129-143.

[53] Guo, F. and Berglund, P., 2017. Transaminase biocatalysis: optimization and application. *Green Chemistry*, *19*(2), pp.333-360.

[54] Stewart, J.D., 2001. Dehydrogenases and transaminases in asymmetric synthesis. *Current opinion in chemical biology*, *5*(2), pp.120-129.

[55] Matcham, G.W. and BOWEN, A.S., 1996. Biocatalysis for chiral intermediates: meeting commercial and technical challenges. *Chimica oggi*, *14*(6), pp.20-24.

[56] Shin, J.S. and Kim, B.G., 1997. Kinetic resolution of α-methylbenzylamine with o-transaminase screened from soil microorganisms: Application of a biphasic system to overcome product inhibition. *Biotechnology and bioengineering*, *55*(2), pp.348-358.

[57] Shin, J.S. and Kim, B.G., 2001. Comparison of the ω-transaminases from different microorganisms and application to production of chiral amines. *Bioscience, biotechnology, and biochemistry*, *65*(8), pp.1782-1788.

[58] Bencze, L.C., Bartha-Vári, J.H., Katona, G., Toşa, M.I., Paizs, C. and Irimie, F.D., 2016. Nanobioconjugates of Candida antarctica lipase B and single-walled carbon nanotubes in biodiesel production. *Bioresource technology*, *200*, pp.853-860.

[59] Bartha-Vári, J.H., Toşa, M.I., Irimie, F.D., Weiser, D., Boros, Z., Vértessy, B.G., Paizs, C. and Poppe, L., 2015. Immobilization of Phenylalanine Ammonia-Lyase on Single-Walled Carbon Nanotubes for Stereoselective Biotransformations in Batch and Continuous-Flow Modes. *ChemCatChem*, *7*(7), p.1122.

[60] Paroul, N., Grzegozeski, L.P., Chiaradia, V., Treichel, H., Cansian, R.L., Oliveira, J.V. and de Oliveira, D., 2011. Solvent-free geranyl oleate production by enzymatic esterification. *Bioprocess and biosystems engineering*, *34*(3), pp.323-329.

[61] Mozingo, R., 2003. Palladium catalysts. *Organic Syntheses*, *26*, pp.77-77.

[62] Kim, M.J., Kim, W.H., Han, K., Choi, Y.K. and Park, J., 2007. Dynamic kinetic resolution of primary amines with a recyclable Pd nanocatalyst for racemization. *Organic letters*, *9*(6), pp.1157-1159.

[63] Boros, Z., Weiser, D., Márkus, M., Abaháziová, E., Magyar, Á., Tomin, A., Koczka, B., Kovács, P. and Poppe, L., 2013. Hydrophobic adsorption and covalent immobilization of Candida antarctica lipase B on mixed-function-grafted silica gel supports for continuous-flow biotransformations. *Process Biochemistry*, *48*(7), pp.1039-1047.

[64] Weiser, D., Nagy, F., Bánóczi, G., Oláh, M., Farkas, A., Szilágyi, A., László, K., Gellért, Á., Marosi, G., Kemény, S. and Poppe, L., 2017. Immobilization engineering–How to design advanced sol–gel systems for biocatalysis?. *Green Chemistry*, *19*(16), pp.3927-3937.

[65] Shin, J.S., Yun, H., Jang, J.W., Park, I. and Kim, B.G., 2003. Purification, characterization, and molecular cloning of a novel amine: pyruvate transaminase from Vibrio fluvialis JS17. *Applied microbiology and biotechnology*, *61*(5), pp.463-471.

[66] Truppo, M.D. and Turner, N.J., 2010. Micro-scale process development of transaminase catalysed reactions. *Organic & biomolecular chemistry*, *8*(6), pp.1280-1283.

[67] Chen, S., Campillo-Brocal, J.C., Berglund, P. and Humble, M.S., 2018. Characterization of the stability of vibrio fluvialis JS17 amine transaminase. *Journal of biotechnology*, *282*, pp.10-17.

[68] Chen, S., Berglund, P. and Humble, M.S., 2018. The effect of phosphate group binding cup coordination on the stability of the amine transaminase from Chromobacterium violaceum. *Molecular Catalysis*, *446*, pp.115-123.

[69] Galman, J.L., Gahloth, D., Parmeggiani, F., Slabu, I., Leys, D. and Turner, N.J., 2018. Characterization of a putrescine transaminase from Pseudomonas putida and its application to the synthesis of benzylamine derivatives. *Frontiers in bioengineering and biotechnology*, *6*, p.205.

[70] Xie, D.F., Fang, H., Mei, J.Q., Gong, J.Y., Wang, H.P., Shen, X.Y., Huang, J. and Mei, L.H., 2018. Improving thermostability of (R)-selective amine transaminase from Aspergillus terreus through introduction of disulfide bonds. *Biotechnology and applied biochemistry*, *65*(2), pp.255-262.

[71] Huang, J., Xie, D.F. and Feng, Y., 2017. Engineering thermostable (R)-selective amine transaminase from Aspergillus terreus through in silico design employing B-factor and folding free energy calculations. *Biochemical and biophysical research communications*, *483*(1), pp.397-402.

[72] Heckmann, C.M., Gourlay, L.J., Dominguez, B. and Paradisi, F., 2020. An (R)-Selective Transaminase From Thermomyces stellatus: Stabilizing the Tetrameric Form. *Frontiers in bioengineering and biotechnology*, *8*, p.707.

[73] Land, H., Campillo-Brocal, J.C., Svendahl Humble, M. and Berglund, P., 2019. B-factor Guided Proline Substitutions in Chromobacterium violaceum Amine Transaminase: Evaluation of the Proline Rule as a Method for Enzyme Stabilization. *ChemBioChem*, *20*(10), pp.1297-1304.

[74] Böhmer, W., Knaus, T., Volkov, A., Slot, T.K., Shiju, N.R., Cassimjee, K.E. and Mutti, F.G., 2019. Highly efficient production of chiral amines in batch and continuous flow by immobilized ω-transaminases on controlled porosity glass metal-ion affinity carrier. *Journal of biotechnology*, *291*, pp.52-60.

[75] Zhang, P., Liao, X., Ma, C., Li, Q., Li, A. and He, Y., 2019. Chemoenzymatic conversion of corncob to furfurylamine via tandem catalysis with tin-based solid acid and transaminase biocatalyst. *ACS Sustainable Chemistry & Engineering*, *7*(21), pp.17636-17642.

[76] Gao, S., Su, Y., Zhao, L., Li, G. and Zheng, G., 2017. Characterization of a (R)-selective amine transaminase from Fusarium oxysporum. *Process Biochemistry*, *63*, pp.130-136.

[77] Yun, H., Hwang, B.Y., Lee, J.H. and Kim, B.G., 2005. Use of enrichment culture for directed evolution of the Vibrio fluvialis JS17 ω-transaminase, which is resistant to product inhibition by aliphatic ketones. *Applied and environmental microbiology*, *71*(8), pp.4220-4224.